Table 2. Serum Lipid profile of pre- and post-pitavastatin treatment

Variable	Patients with dyslipidemia (n=30) pre	Patients with dyslipidemia (n=30) post	p value
Serum concentration Cholesterol (mg/dL)			
Total-C(mg/dL)	224.4±40.1	165.5±28.4	≤0.01
HDL-C (mg/dL)	50.7±11.4	55.3±11.4	≤0.01
LDL-C (mg/dL)	146.3±31.7	89.6±18.6	≤0.01
Triglycerides (mg/dL)	152.7±100.3	123.7±64.2	0.02
Median	118	109	
Interquartile range	60-454	46-313	
Apolipoprotein (mg/dL)			
apoA-I (mg/dL)	120.0±31.5	124.4±35.5	0.16
Phospholipid (mg/dL)			
Total-PL (mg/dL)	190.9±30.3	168.6±22.3	≤0.01
HDL fraction			
apoA-I (mg/dL)	69.3±24.8	73.4±31.2	0.52
apoA-II (mg/dL)	13.0±7.3	12.4±4.2	0.67
apoE (mg/dL)	1.82±1.21	1.25±0.57	0.053
HDL-PL (mg/dL)	117.3±43.6	145.2±58.6	0.047
FC/CE ratio	0.17±0.06	0.17±0.05	0.75

Total-C; total-cholesterol, HDL-C; high density lipoprotein-cholesterol, LDL-C; low density lipoproteincholesterol, apoA-I; apolipoprotein A-I, PL; phospholipid, FC; free cholesterol, CE; cholesteryl ester, HDL fraction was purified with polyethylene glycol precipitation. data represent mean±SD

measured using a commercially available ELISA kit (ASSAYPRO, MO, USA). The lipoprotein profiles were determined using HPLC (LipoSEARCH®) at Skylight Biotech, Inc. (Akita, Japan), according to the specified procedure[21]. The levels of HDL-phospholipids, total cholesterol (TC), and free cholesterol (FC) were measured with PEG-HDL using a commercially available kit from WAKO (Osaka, Japan). The level of HDL-cholesteryl ester (CE) was calculated by subtracting the level of HDL-FC from the level of HDL-TC.

Cholesterol Efflux Study

The cholesterol efflux studies were performed as previously described[18]. The human monocyte cell line THP-1 (RIKEN, Tsukuba, Japan) was cultured in RPMI 1640 medium (Wako, Osaka, Japan) containing 10% fetal bovine serum. The cells were harvested in 24-well plates and differentiated into macrophages using 200 nmol/L of phorbor myristate acetate (Sigma-Aldrich, MO, USA) for 72 hours. Next, the adherent macrophages were incubated with 25 μg/mL of acetyl LDL and 1 μCi of [^{3}H] cholesterol (Perkin-Elmer Life Science, MA, USA) for 24 hours, followed by treatment with 10 μmol/L of Liver X receptor agonist TO901317 (Sigma-Aldrich, MO, USA) for 16 hours. The cells were then incubated with either 2.8% PEG-HDL or PEG-PBS in RPMI 1640 medium with 0.2% bovine serum albumin for four hours to induce cholesterol efflux. The percent efflux capacity was calculated according to the following formula: (DPM of [^{3}H] cholesterol in media containing 2.8% PEG-HDL) ÷ [(DPM of [^{3}H] cholesterol in media containing 2.8% PEG-HDL) + (DPM of [^{3}H] cholesterol in cells extracted after efflux study)] × 100. The PEG-HDL-specific efflux capacity was calculated according to the following formula: [(% cholesterol efflux by 2.8% PEG-HDL) − (% cholesterol efflux by PEG-PBS)].

PON-1 and PAF-AH Activities

The PON-1 activity was analyzed spectrophotometrically with PEG-HDL (HDL-associated PON-1), as previously reported[22]. Two individual PON-1 activities were evaluated. The paraoxonase activity was measured with paraoxon (Sigma-Aldrich, MO, USA) as a substrate, whereas the arylesterase activity was measured with phenylacetate (Sigma-Aldrich, MO, USA) as a substrate. The HDL-associated PAF-AH activity was measured using a commercially available kit (Cayman Chemicals, MI, USA).

Statistical Analysis

All values are presented as the mean±SD. Comparisons between the parameters of pre- and post-pitavastatin treatment were made with paired Stu-

dent's *t*-test (two-tailed) using the GraphPad Prism Software program.

Results

Pitavastatin Increased the Serum HDL-C and HDL-Phospholipids Levels

The lipid profiles of the patients (**Table 1**) pre- and post-pitavastatin treatment are shown in **Table 2**. Pitavastatin significantly decreased the serum Total-C, LDL-C and TG levels and increased the serum HDL-C levels in the dyslipidemic patients by 9% compared to the baseline values. Pitavastatin treatment led to a significant increase in the phospholipid content of the HDL fraction of 7.8%. The HPLC analysis revealed that the peak HDL fraction deviated to the left, indicating an increase in the number of large HDL particles (**Fig. 1A, B**). The levels of ApoA-I, apoA-II and apoE and the FC/CE ratio of HDL did not change during pitavastatin treatment. Taken together, pitavastatin increased the number of phospholipid-rich large HDL particles without modifying the apolipoprotein distribution.

Pitavastatin Increased the Serum Cholesterol Efflux Capacity

The cholesterol efflux capacity of HDL isolated via PEG precipitation was performed using THP-1 macrophages incubated with acetyl LDL and the Liver X receptor agonist in order to mimic the macrophage phenotypes in atherosclerotic lesions. We confirmed that TO901317 treatment increased the mRNA expressions of ATP-binding cassette transporter A1 (ABCA1) and G1 (ABCG1), while acetyl LDL treatment decreased the scavenger receptor class B type I (SR-BI) mRNA expression in THP-1 macrophages (data not shown). Pitavastatin significantly increased the PEG-HDL-specific cholesterol efflux capacity in the dyslipidemic patients by 8.6% (6.6±1.4 vs 7.1±1.7%; $p<0.05$) (**Fig. 2A, 2B**). The cholesterol efflux capacity standardized according to the serum apoA-I level was increased during pitavastatin treatment (**Fig. 2**), indicating that the increased HDL level contributed to the increased efflux capacity. These findings suggest that pitavastatin increases the amount of HDL particles that are functionally preserved with a cholesterol efflux capacity.

Pitavastatin Enhanced Serum Antioxidant Properties

The PON-1 activity is widely used to evaluate the antioxidant properties of HDL[6, 23, 24]. Therefore, the HDL-associated PON-1 activities in the pre- and post-pitavastatin serum samples were measured. The

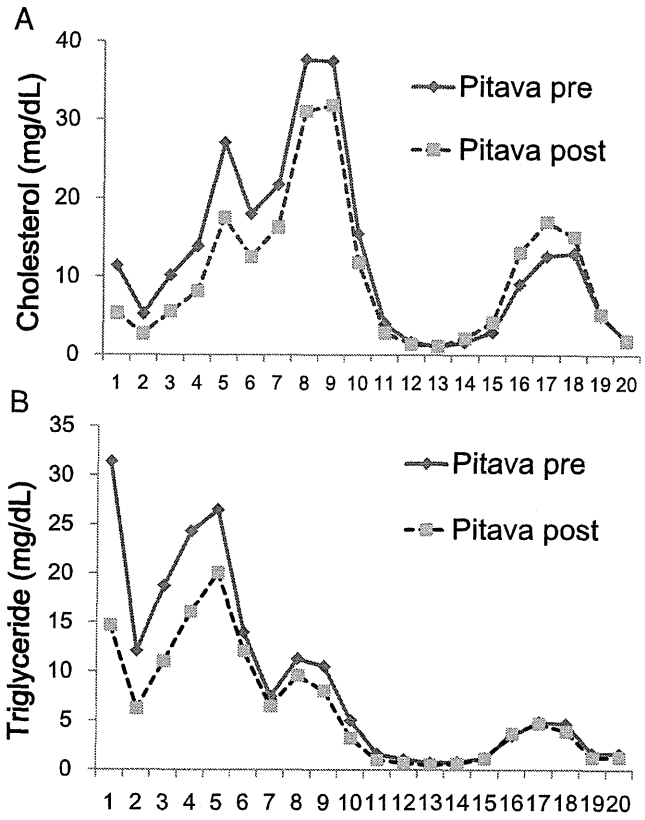

Fig. 1. Effects of pitavastatin treatment on lipoprotein profiles evaluated using HPLC.

The serum samples of dyslipidemic patients were subjected to HPLC. Fractions 1,2: Chylomicron remnant, 3-7: very-low-density lipoprotein, 8-13: low-density lipoprotein, 14-20: high-density lipoprotein A. HPLC profiles of the cholesterol levels (mg/dL). B. HPLC profiles of the triglyceride levels (mg/dL).

HDL-associated paraoxonase activity was increased in the dyslipidemic patients by 9% (23.2±9.7 vs 25.0±10.5 pmol/min/mL PEG-HDL; $p<0.05$) (**Fig. 3A, 3B**). The HDL-associated arylesterase activity was increased by 11% (58.7±20 vs 63.1±19 pmol/min/mL PEG-HDL; $p<0.05$) (**Fig. 3C, 3D**). Neither the HDL-associated paraoxonase or arylesterase activity standardized according to the serum apoA-I level changed during pitavastatin treatment (data not shown). Similarly, the HDL-associated PAF-AH activity did not change during pitavastatin treatment (71.5±21.2 vs 71.2±25.6 pmol/min/mL PEG-HDL; $p=0.92$) (**Fig. 4A, 4B**). These data suggest that pitavastatin enhances serum antioxidant properties by increasing the number of HDL particles that possess PON-1 activities.

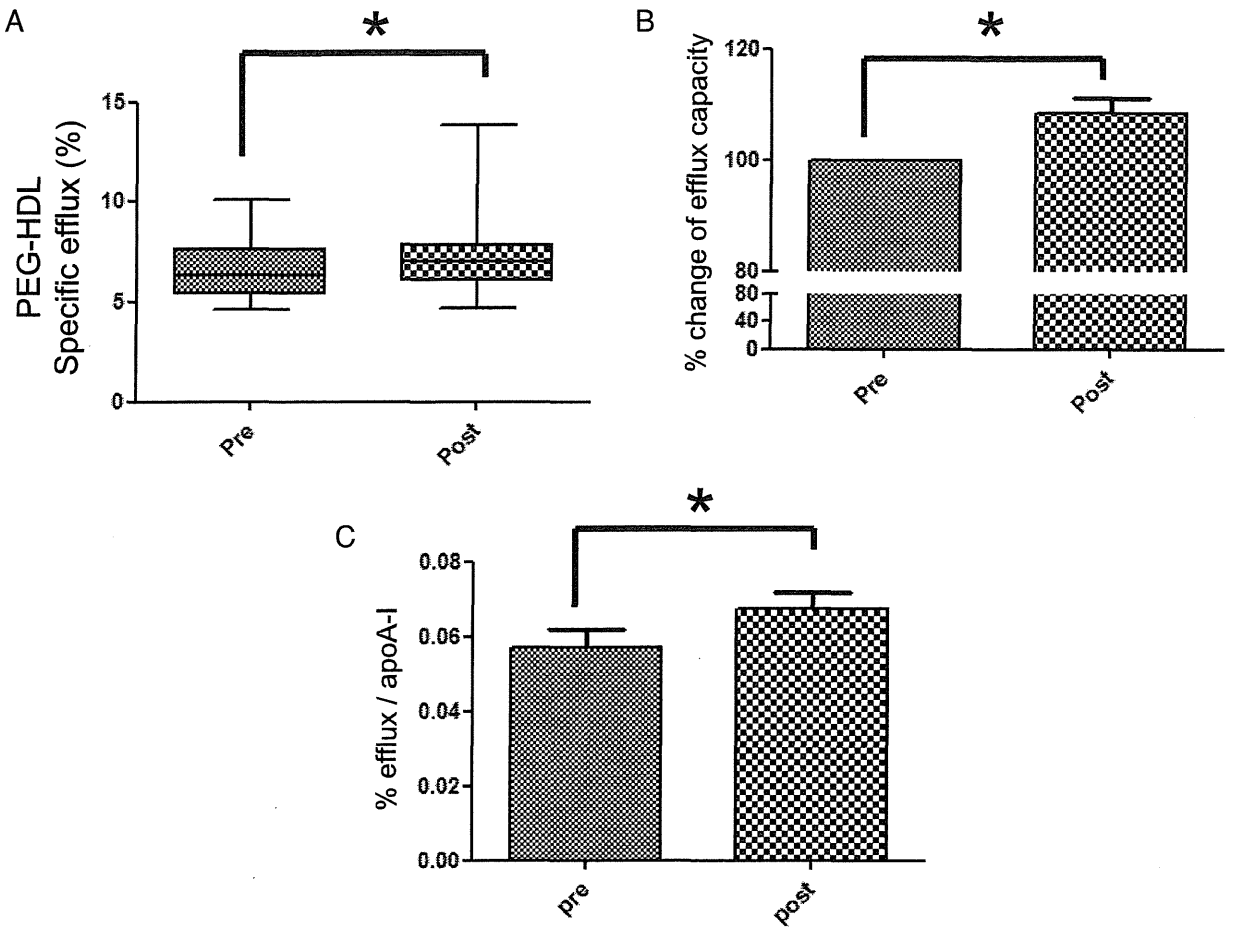

Fig. 2. Effects of pitavastatin treatment on PEG-HDL-specific cholesterol efflux in the dyslipidemic patients.

A. The cholesterol efflux capacity induced by the same volume of 2.8% PEG-HDL in TO901317-treated THP-1 macrophages pre- and post-pitavastatin treatment. B. The percent change in the PEG-HDL-specific cholesterol efflux capacity pre- and post-pitavastatin treatment. C. The cholesterol efflux induced by the same volume of 2.8% PEG-HDL standardized according to the serum apoA-I level pre- and post-pitavastatin treatment. The bars represent the mean ± SEM. $^{*}p < 0.05$

Discussion

Although a large number of epidemiological studies have documented a strong inverse association between the plasma HDL-C level and the incidence of cardiovascular events, the benefits of HDL-raising pharmaceutical intervention remain controversial[7, 25]. The relationship between the plasma HDL-C level and the risk of cardiovascular events is often explained by the functional quality of HDL, including cholesterol efflux and the antioxidative, anti-inflammatory and antiproliferative properties[6]. Cholesterol efflux from macrophages is the rate-limiting first step in RCT from a diseased vessel wall to the liver. A recent study demonstrated that the cholesterol efflux capacity of HDL is an independent negative risk factor for CAD[26]. Additionally, Patel *et al.* reported that the antioxidative capacity of HDL, as evaluated in a cell-free assay, is attenuated in patients with acute coronary syndrome[27]. Therefore, changes in the quality of functional HDL are closely related to the risk of cardiovascular disease. In this study, pitavastatin treatment increased the cholesterol efflux capacity and the PON-1 activity in association with antioxidant properties in conditioned HDL isolated from dyslipidemic patients. These effects occurred in parallel with an increase in the serum HDL-C level. Taken together, pitavastatin increased the amount of functional HDL without attenuating the HDL quality.

Several plausible explanations have been proposed for the molecular mechanisms underlying the effects of pitavastatin on HDL. Previous studies have indicated that pitavastatin increases apoA-I production both *in vitro*[14] and *in vivo*[28]. In addition,

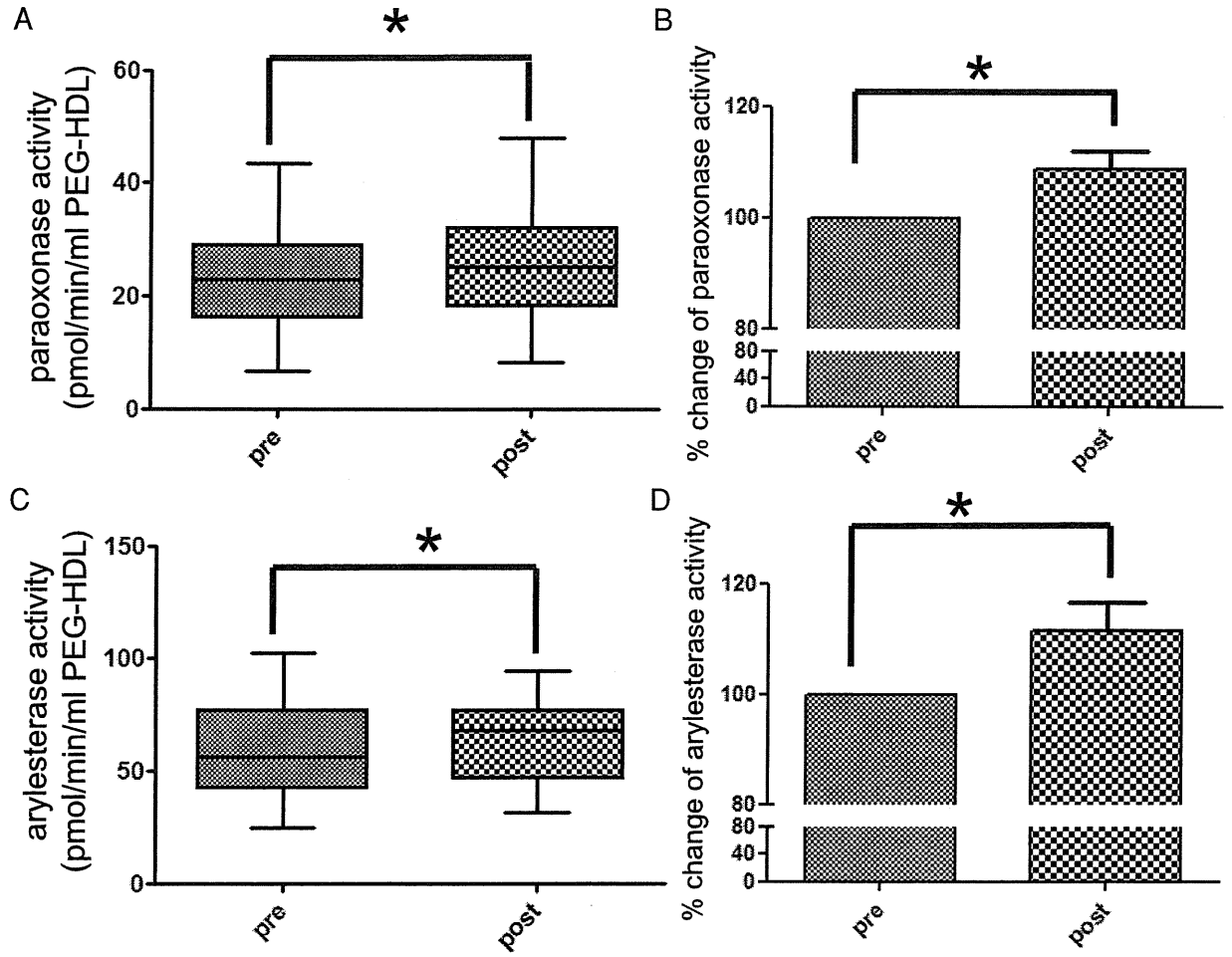

Fig. 3. Effects of pitavastatin treatment on the paraoxonase activity in the dyslipidemic patients.

A. The paraoxonase activity of the same volume of PEG-HDL (=HDL-associated paraoxonase activity) pre- and post-pitavastatin treatment. B. The percent change in the paraoxonase activity pre- and post-pitavastatin treatment. C. The arylesterase activity of the same volume of PEG-HDL (=HDL-associated arylesterase activity) pre- and post-pitavastatin treatment. D. The percent change in the arylesterase activity pre- and post-pitavastatin treatment. The bars represent the mean ± SEM. $^{*}p<0.05$

pitavastatin has been reported to increase the ABCA1 expression *in vitro*[29]. Pitavastatin also decreases the expression of endothelial lipase, which increases not only the quantity of HDL, but also the HDL particle size by increasing the amount of phospholipid content[16]. The phospholipid-rich HDL particles generated by EL suppression exert anti-inflammatory and antioxidative effects[22]. As for cholesterol efflux, in the macrophages used in the efflux method in this study, both ABCA1 and ABCG1 were upregulated by the LXR agonist, and SR-BI was downregulated by acetyl LDL treatment. The macrophages ABCA1 and ABCG1 play crucial roles in *in vivo* reverse cholesterol transport[30]. ABCA1 primarily promotes cholesterol efflux through the actions of lipid-poor apoA-I and nascent HDL, whereas ABCG1 and SR-BI mediate efflux through the actions of mature HDL[31]. Given that pitavastatin increases the amount of mature phospholipid-rich HDL and decreases the amount of nascent pre-beta HDL[15], we speculate that the increased level of mature HDL induced by pitavastatin contributes to enhancing the efflux capacity, most likely via the actions of ABCG1. In brief, pitavastatin increases the amount of HDL via a dual mechanism through which it attenuates HDL catabolism and promotes HDL synthesis.

Khera *et al.* recently reported that statin treatment did not increase the serum cholesterol efflux capacity in their cohort study[26]. However, the serum cholesterol efflux capacity was measured at only one time point and pitavastatin was not included in the medication regimen. Pitavastatin has a greater capacity

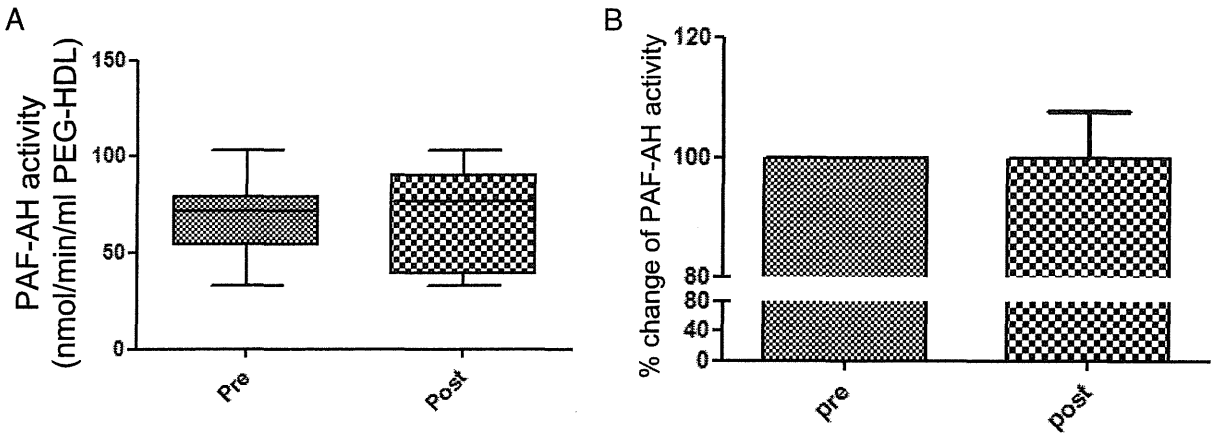

Fig. 4. Effects of pitavastatin treatment on the PAF-AH activity in the dyslipidemic patients.

A. The PAF-AH activity of the same volume of PEG-HDL (=HDL-associated PAF-AH activity) pre- and post-pitavastatin treatment. B. The percent change in the HDL-associated PAF-AH activity pre- and post-pitavastatin treatment. The bars represent the mean ± SEM.

to increase the HDL-C level than other statins[13], and the present study directly assessed changes in the efflux capacity pre- and post-pitavastatin treatment.

PON-1 is an HDL-associated protein that exerts antioxidative effects on HDL. The PON-1 activity is evaluated using several individual substrates. The substrate of the paraoxonase activity assay is paraoxon, while that of the arylesterase activity assay is phenylacetate, and there is a positive relationship between the results of these assays[22]. Previous studies have shown that statins increase the PON-1 mass and activity by up to 40%[32]. In the present study, pitavastatin increased the HDL associated-paraoxonase activity by 10% and the HDL associated-arylesterase activity by 14%, which dominated the increased serum HDL-C level. This finding may be partially due to the fact that pitavastatin directly upregulates the PON-1 expression in cultured hepatocytes[33].

In this study, we selected pitavastatin because it has a greater capacity to raise the HDL level than other statins; however, the HDL-raising effects of pitavastatin are shared by other statins[10]. Clinical studies of both pravastatin[34] and rosuvastatin[35] have shown that regression of the atherosclerotic plaque volume is positively correlated with changes in the HDL-C level. Combining these clinical data with our results, the raised HDL level observed during statin therapy may be beneficial for reducing the amount of atherosclerotic lesions by increasing the cholesterol efflux capacity and antioxidant properties.

It has not been elucidated yet whether the statin-induced changes observed in the HDL antiatherogenic properties are physiologically relevant to preventing the progression of atherosclerosis, although both the cholesterol efflux capacity and the PON-1 activity are correlated with the prevalence of atherosclerosis[23, 26]. In the present study, changes in the cholesterol efflux capacity were not correlated with changes in the PON-1 activity (data not shown). Furthermore, the activity of another antioxidant enzyme, PAF-AH, was not affected by pitavastatin. Previous reports have also shown that the cholesterol efflux capacity is not always associated with antioxidant properties[26, 27]. These findings indicate that each parameter representing HDL antiatherosclerotic properties is independent, and further studies are needed to identify the most important and relevant markers of the quality of functional HDL.

The results of clinical trials of CETP inhibitors are confusing with respect to HDL-raising therapies. Two CETP inhibitors, torcetrapib[7] and dalcetrapib[36], failed to reduce the incidence of cardiovascular events despite raising the HDL-C levels. It has been reported that the HDL elevated by CETP inhibition or deficiency possesses normal or enhanced cholesterol efflux[37] and antioxidant properties[38], indicating that dysfunctional HDL does not affect the overall results. In general, statins inhibit the CETP activity[10], and the increased HDL level induced by statins may be partially due to CETP inhibition. Therefore, both statins and CETP inhibitors increase the amount of functionally preserved HDL. However, there is a large discrepancy in clinical outcomes between statins and CETP inhibitors, the precise mechanisms of which remain unknown. These data imply that raising the level of functional HDL via pharmaceutical intervention alone does not lead to improved clinical out-

comes in patients with cardiovascular disease. Clinical studies of two other novel CETP inhibitors are currently ongoing, the results of which may provide additional insight.

Several limitations are associated with the present study. This study consisted of a small number of subjects, and we did not compare the effects of pitavastatin with those of other statins. In addition, the duration of pitavastatin treatment was not long, although several clinical studies have shown that pitavastatin treatment increases the HDL level by over 10% for longer periods[12, 16]. In our study cohort, few participants exhibited low levels of HDL-C, and the effects of statins may have been greater if the study was conducted among low HDL-C patients only. Further studies should be performed to evaluate these issues.

In conclusion, pitavastatin treatment increases the serum HDL-C levels in association with increases in the cholesterol efflux capacity and PON-1 activity in dyslipidemic patients. In general, pitavastatin increases the amount of HDL particles while functionally preserving antiatherosclerotic properties. The increased quantity and quality of HDL may at least, in part, contribute to the antiatherosclerotic effects of this statin.

Sources of Funding

This study was supported by a grant for scientific research from the Ministry of Education, Culture, Sports, Science and Technology (MEXT) of Japan.

Abbreviations

HDL-C; high density lipoprotein, LDL; low density lipoprotein, TG; triglyceride, CETP; cholesteryl ester transfer protein, PON-1; paraoxonase-1, PAF-AH; platelet-activating factor acetylhydrolase, RCT; reverse cholesterol transport, CAD; coronary artery disease, apoA-I; apolipoprotein A-I, apoA-II; apolipoprotein A-II, apoB; apolipoprotein B, ABCA1; ATP-binding cassette transporter A1, ABCG1; ATP-binding cassette transporter G1, SR-BI; scavenger receptor class B type I, PEG; polyethethylene glycol, EL; endothelial lipase

Conflicts of Interest

None.

References

1) Baigent C, Blackwell L, Emberson J, Holland LE, Reith C, Bhala N, Peto R, Barnes EH, Keech A, Simes J, Collins R: Efficacy and safety of more intensive lowering of LDL cholesterol: A meta-analysis of data from 170,000 participants in 26 randomised trials. Lancet, 2010; 376: 1670-1681
2) Mora S, Wenger NK, Demicco DA, Breazna A, Boekholdt SM, Arsenault BJ, Deedwania P, Kastelein JJ, Waters DD: Determinants of residual risk in secondary prevention patients treated with high- versus low-dose statin therapy: The treating to new targets (tnt) study. Circulation, 2012; 125: 1979-1987
3) Castelli WP: Cholesterol and lipids in the risk of coronary artery disease--the framingham heart study. Can J Cardiol, 1988; 4 Suppl A: 5A-10A
4) Barter P, Gotto AM, LaRosa JC, Maroni J, Szarek M, Grundy SM, Kastelein JJ, Bittner V, Fruchart JC: HDL cholesterol, very low levels of LDL cholesterol, and cardiovascular events. N Engl J Med, 2007; 357: 1301-1310
5) Rader DJ, Alexander ET, Weibel GL, Billheimer J, Rothblat GH: The role of reverse cholesterol transport in animals and humans and relationship to atherosclerosis. J Lipid Res, 2009; 50 Suppl: S189-194
6) Barter PJ, Nicholls S, Rye KA, Anantharamaiah GM, Navab M, Fogelman AM: Antiinflammatory properties of HDL. Circ Res, 2004; 95: 764-772
7) Barter PJ, Caulfield M, Eriksson M, Grundy SM, Kastelein JJ, Komajda M, Lopez-Sendon J, Mosca L, Tardif JC, Waters DD, Shear CL, Revkin JH, Buhr KA, Fisher MR, Tall AR, Brewer B: Effects of torcetrapib in patients at high risk for coronary events. N Engl J Med, 2007; 357: 2109-2122
8) Navab M, Anantharamaiah GM, Reddy ST, Van Lenten BJ, Ansell BJ, Fogelman AM: Mechanisms of disease: Proatherogenic HDL--an evolving field. Nat Clin Pract Endocrinol Metab, 2006; 2: 504-511
9) Navab M, Reddy ST, Van Lenten BJ, Anantharamaiah GM, Fogelman AM: The role of dysfunctional HDL in atherosclerosis. J Lipid Res, 2009; 50 Suppl: S145-149
10) Yamashita S, Tsubakio-Yamamoto K, Ohama T, Nakagawa-Toyama Y, Nishida M: Molecular mechanisms of HDL-cholesterol elevation by statins and its effects on HDL functions. J Atheroscler Thromb, 2010; 17: 436-451
11) Fukutomi T, Takeda Y, Suzuki S, Ito T, Joh T, Itoh M: High density lipoprotein cholesterol and apolipoprotein A-I are persistently elevated during long-term treatment with pitavastatin, a new HMG-CoA reductase inhibitor. Int J Cardiol, 2010; 141: 320-322
12) Teramoto T, Shimano H, Yokote K, Urashima M: Effects of pitavastatin (livalo tablet) on high density lipoprotein cholesterol (HDL-c) in hypercholesterolemia. J Atheroscler Thromb, 2009; 16: 654-661
13) Maruyama T, Takada M, Nishibori Y, Fujita K, Miki K, Masuda S, Horimatsu T, Hasuike T: Comparison of preventive effect on cardiovascular events with different statins. -the CIRCLE study. Circ J, 2011; 75: 1951-1959
14) Maejima T, Yamazaki H, Aoki T, Tamaki T, Sato F, Kitahara M, Saito Y: Effect of pitavastatin on apolipoprotein A-I production in hepg2 cell. Biochem Biophys Res Commun, 2004; 324: 835-839
15) Kawano M, Nagasaka S, Yagyu H, Ishibashi S: Pitavas-

tatin decreases plasma prebeta1-HDL concentration and might promote its disappearance rate in hypercholesterolemic patients. J Atheroscler Thromb, 2008; 15: 41-46
16) Kojima Y, Ishida T, Sun L, Yasuda T, Toh R, Rikitake Y, Fukuda A, Kume N, Koshiyama H, Taniguchi A, Hirata K: Pitavastatin decreases the expression of endothelial lipase both in vitro and in vivo. Cardiovasc Res, 2010; 87: 385-393
17) Teramoto T, Sasaki J, Ueshima H, Egusa G, Kinoshita M, Shimamoto K, Daida H, Biro S, Hirobe K, Funahashi T, Yokote K, Yokode M: Diagnostic criteria for dyslipidemia. Executive summary of Japan atherosclerosis society (JAS) guideline for diagnosis and prevention of atherosclerotic cardiovascular diseases for Japanese. J Atheroscler Thromb, 2007; 14: 155-158
18) Yvan-Charvet L, Kling J, Pagler T, Li H, Hubbard B, Fisher T, Sparrow CP, Taggart AK, Tall AR: Cholesterol efflux potential and antiinflammatory properties of high-density lipoprotein after treatment with niacin or anacetrapib. Arterioscler Thromb Vasc Biol, 2010; 30: 1430-1438
19) Schissel SL, Tweedie-Hardman J, Rapp JH, Graham G, Williams KJ, Tabas I: Rabbit aorta and human atherosclerotic lesions hydrolyze the sphingomyelin of retained low-density lipoprotein. Proposed role for arterial-wall sphingomyelinase in subendothelial retention and aggregation of atherogenic lipoproteins. J Clin Invest, 1996; 98: 1455-1464
20) Basu SK, Goldstein JL, Anderson GW, Brown MS: Degradation of cationized low density lipoprotein and regulation of cholesterol metabolism in homozygous familial hypercholesterolemia fibroblasts. Proc Natl Acad Sci U S A, 1976; 73: 3178-3182
21) Usui S, Hara Y, Hosaki S, Okazaki M: A new on-line dual enzymatic method for simultaneous quantification of cholesterol and triglycerides in lipoproteins by HPLC. J Lipid Res, 2002; 43: 805-814
22) Hara T, Ishida T, Kojima Y, Tanaka H, Yasuda T, Shinohara M, Toh R, Hirata K: Targeted deletion of endothelial lipase increases HDL particles with anti-inflammatory properties both in vitro and in vivo. J Lipid Res, 2011; 52: 57-67
23) Mackness B, Durrington P, McElduff P, Yarnell J, Azam N, Watt M, Mackness M: Low paraoxonase activity predicts coronary events in the caerphilly prospective study. Circulation, 2003; 107: 2775-2779
24) Van Lenten BJ, Hama SY, de Beer FC, Stafforini DM, McIntyre TM, Prescott SM, La Du BN, Fogelman AM, Navab M: Anti-inflammatory HDL becomes pro-inflammatory during the acute phase response. Loss of protective effect of HDL against LDL oxidation in aortic wall cell cocultures. J Clin Invest, 1995; 96: 2758-2767
25) Duffy D, Rader DJ: Update on strategies to increase HDL quantity and function. Nat Rev Cardiol, 2009; 6: 455-463
26) Khera AV, Cuchel M, de la Llera-Moya M, Rodrigues A, Burke MF, Jafri K, French BC, Phillips JA, Mucksavage ML, Wilensky RL, Mohler ER, Rothblat GH, Rader DJ: Cholesterol efflux capacity, high-density lipoprotein function, and atherosclerosis. N Engl J Med, 2011; 364: 127-135
27) Patel PJ, Khera AV, Jafri K, Wilensky RL, Rader DJ: The anti-oxidative capacity of high-density lipoprotein is reduced in acute coronary syndrome but not in stable coronary artery disease. J Am Coll Cardiol, 2011; 58: 2068-2075
28) Sasaki J, Ikeda Y, Kuribayashi T, Kajiwara K, Biro S, Yamamoto K, Ageta M, Kobori S, Saikawa T, Otonari T, Kono S: A 52-week, randomized, open-label, parallel-group comparison of the tolerability and effects of pitavastatin and atorvastatin on high-density lipoprotein cholesterol levels and glucose metabolism in Japanese patients with elevated levels of low-density lipoprotein cholesterol and glucose intolerance. Clin Ther, 2008; 30: 1089-1101
29) Kobayashi M, Gouda K, Chisaki I, Ochiai M, Itagaki S, Iseki K: Regulation mechanism of ABCA1 expression by statins in hepatocytes. Eur J Pharmacol, 2011; 662: 9-14
30) Wang X, Collins HL, Ranalletta M, Fuki IV, Billheimer JT, Rothblat GH, Tall AR, Rader DJ: Macrophage ABCA1 and ABCG1, but not SR-BI, promote macrophage reverse cholesterol transport in vivo. J Clin Invest, 2007; 117: 2216-2224
31) Yancey PG, Kawashiri MA, Moore R, Glick JM, Williams DL, Connelly MA, Rader DJ, Rothblat GH: In vivo modulation of HDL phospholipid has opposing effects on SR-BI- and ABCA1-mediated cholesterol efflux. J Lipid Res, 2004; 45: 337-346
32) Harangi M, Seres I, Harangi J, Paragh G: Benefits and difficulties in measuring HDL subfractions and human paraoxonase-1 activity during statin treatment. Cardiovasc Drugs Ther, 2009; 23: 501-510
33) Ota K, Suehiro T, Arii K, Ikeda Y, Kumon Y, Osaki F, Hashimoto K: Effect of pitavastatin on transactivation of human serum paraoxonase 1 gene. Metabolism, 2005; 54: 142-150
34) Tani S, Watanabe I, Anazawa T, Kawamata H, Tachibana E, Furukawa K, Sato Y, Nagao K, Kanmatsuse K, Kushiro T: Effect of pravastatin on malondialdehyde-modified low-density lipoprotein levels and coronary plaque regression as determined by three-dimensional intravascular ultrasound. Am J Cardiol, 2005; 96: 1089-1094
35) Takayama T, Hiro T, Yamagishi M, Daida H, Hirayama A, Saito S, Yamaguchi T, Matsuzaki M: Effect of rosuvastatin on coronary atheroma in stable coronary artery disease: Multicenter coronary atherosclerosis study measuring effects of rosuvastatin using intravascular ultrasound in Japanese subjects (cosmos). Circ J, 2009; 73: 2110-2117
36) Schwartz GG, Olsson AG, Abt M, Ballantyne CM, Barter PJ, Brumm J, Chaitman BR, Holme IM, Kallend D, Leiter LA, Leitersdorf E, McMurray JJ, Mundl H, Nicholls SJ, Shah PK, Tardif JC, Wright RS: Effects of dalcetrapib in patients with a recent acute coronary syndrome. N Engl J Med, 2012; 367: 2089-2099
37) Yvan-Charvet L, Matsuura F, Wang N, Bamberger MJ, Nguyen T, Rinninger F, Jiang XC, Shear CL, Tall AR: Inhibition of cholesteryl ester transfer protein by torcetrapib modestly increases macrophage cholesterol efflux to HDL. Arterioscler Thromb Vasc Biol, 2007; 27: 1132-1138
38) Chantepie S, Bochem AE, Chapman MJ, Hovingh GK, Kontush A: High-density lipoprotein (HDL) particle subpopulations in heterozygous cholesteryl ester transfer protein (cetp) deficiency: Maintenance of antioxidative activity. PLoS One, 2012; 7: e49336

Biochemical and Biophysical Research Communications 440 (2013) 521–526

Contents lists available at ScienceDirect

Biochemical and Biophysical Research Communications

journal homepage: www.elsevier.com/locate/ybbrc

A novel link between *Slc22a18* and fat accumulation revealed by a mutation in the spontaneously hypertensive rat

Takashi Yamamoto [a,b], Kozue Izumi-Yamamoto [a,b], Yoko Iizuka [c], Midori Shirota [a,b], Miki Nagase [b], Toshiro Fujita [d], Takanari Gotoda [a,b,*]

[a] Department of Clinical and Molecular Epidemiology, 22nd Century Medical and Research Center, The University of Tokyo, Tokyo 113-8655, Japan
[b] Department of Nephrology and Endocrinology, The University of Tokyo, Tokyo 113-8655, Japan
[c] Department of Diabetes and Metabolic Disease, The University of Tokyo, Tokyo 113-8655, Japan
[d] Division of Clinical Epigenetics, Research Center for Advanced Science and Technology, The University of Tokyo, Tokyo 153-8904, Japan

ARTICLE INFO

Article history:
Received 15 September 2013
Available online 4 October 2013

Keywords:
SHR
QTL
Cd36
Solute carrier
Adipocyte differentiation
Obesity

ABSTRACT

Two different strains of the spontaneously hypertensive rat (SHR) exist, either with or without a *Cd36* mutation. In the F2 population derived from a cross between these two SHR strains, the mutant *Cd36* allele was tightly linked to differences in metabolic phenotypes but not to those in fat pad weight. This suggested the existence of another crucial mutation related to adiposity. Linkage analysis of this F2 population showed a significant linkage between the rat chromosome 1 region (*D1Rat240–D1Wox28*) and fat pad weight. By integrating both positional and expression information, we identified a donor splice site mutation in the gene for solute carrier family 22 member 18 (Slc22a18) in SHR with reduced fat pad weight. This mutation was located at the linkage peak with a maximum logarithm of odds score of 7.7 and caused skipping of the whole exon 9 that results in a complete loss of a whole membrane-spanning region of the rat Slc22a18 protein. *Slc22a18* mRNA was abundantly expressed in isolated adipocytes and in a differentiation-dependent manner in 3T3-L1 cells. Knockdown of the *Slc22a18* mRNA via infection of adenoviral vectors markedly inhibited both triglyceride accumulation and adipocyte differentiation in 3T3-L1 cells. By contrast, overexpression of the *Slc22a18* mRNA had the opposite effects. These results reveal a novel link between *Slc22a18* and fat accumulation and suggest that this gene could be a new therapeutic target in obesity.

1. Introduction

The spontaneously hypertensive rat (SHR) is a widely-used animal model of essential hypertension and demonstrates a series of manifestations of insulin resistance syndrome [1]. We previously reported that there were two different SHR strains, depending on the presence or absence of a *de novo* mutation in the gene for Cd36, and that they manifested significant differences in several important phenotypes [2]. The SHR strain with a *Cd36* null mutation (hereafter referred to as SHR/NCrj) had significantly reduced blood glucose and triglyceride levels and increased blood free fatty acid levels as compared with the SHR strain without this mutation (referred to as SHR/Izm). Furthermore, the SHR/NCrj strain also showed markedly decreased epididymal fat pad weight as compared with the SHR/Izm strain, although both SHR strains had comparable body weights [2].

Cd36 is a multi-functional transporter that is involved in glucose and lipid metabolism and is known to facilitate the uptake of long-chain fatty acids in adipocytes [3]. Taking into consideration the known function of Cd36 and the extreme genetic similarity between these two SHR strains, we hypothesised that the phenotypic differences observed between these two strains could be attributable to a *Cd36* mutation.

In the present study, we initially examined for possible linkages between the mutant *Cd36* allele and the respective phenotypes in an F2 population derived from a cross between these SHR strains. Comparing these relatively identical strains provides a unique opportunity for linkage analysis with minimal effects of genetic noise. In this F2 cross, as expected, the mutant *Cd36* allele was significantly linked to altered metabolic phenotypes, but unexpectedly, not to the differences in fat pad weight, which strongly suggested another crucial mutation underling the differences in adiposity between these two rat strains. Based on the results of linkage and mRNA expression analyses, we report a novel link between solute carrier family 22 member 18 (Slc22a18) and fat accumulation.

* Corresponding author at: Department of Clinical and Molecular Epidemiology, 22nd Century Medical and Research Center, The University of Tokyo Hospital, 7-3-1 Hongo, Tokyo 113-8655, Japan. Fax: +81 3 5800 9169.
E-mail address: gotoda-tky@umin.ac.jp (T. Gotoda).

0006-291X/$ - see front matter © 2013 Elsevier Inc. All rights reserved.
http://dx.doi.org/10.1016/j.bbrc.2013.09.096

2. Materials and methods

2.1. Animals

NCrj rat strains were purchased from Charles River (Japan) and Izm strains were from Funabashi Farm (Chiba, Japan). All rats were maintained under stable conditions on a 12-h light–dark cycle and fed standard laboratory chow (MF purchased from Oriental Yeast, Ltd., Japan) and water ad libitum. At 12 weeks of age, after measuring its body weight, a male rat was sacrificed after an overnight fast. Arterial blood and tissue samples were collected rapidly, frosen in liquid nitrogen, and kept at −80 °C prior to analyses. Whole blood glucose levels were measured using a glucometer (Sankyo, Japan), and serum cholesterol and free fatty acid levels were determined by enzymatic assays (Kyowa, Japan). All animal procedures were performed in accordance with the guidelines for the care and use of laboratory animals approved by University of Tokyo Graduate School of Medicine.

2.2. Isolation of genomic DNA, genotyping, and DNA sequencing

DNA was isolated from a whole blood sample of each rat with a DNA extractor WB kit (WAKO, Japan). DNA (100 ng) was used for polymerase chain reaction (PCR) as previously described [4]. The resulting PCR products were analysed with 1–4% NuSieve 3:1 agarose gels (Takara Bio, Japan) or with a GenePhor DNA Separation System (GE Healthcare) for single strand conformation polymorphism (SSCP) analysis. A polymorphic (CA)*n*-repeat site was found 13-bases downstream of the *Slc22a18* mutation site, and tight linkage was observed between the wild-type G allele and $(CA)_{18}$ and between the mutant A allele and $(CA)_{28}$ (Supplementary Table 1). PCR was run with a pair of primers (upstream: 5′-CTGCTGAGATCCAGTGTACT-3′, downstream: 5′-TGGAGGATGGCTTGAGACCT-3′) that spanned both the mutation and (CA)*n*-repeat sites, which generated PCR-products of 142 base-pairs (bp) for the wild-type allele and of 162 bp for the mutant allele. Genotyping of the *Cd36* mutation was performed as previously described [2]. Genotyping for 11 other polymorphic microsatellite markers (*D1Wox32*, *D1Rat240*, *D1Wox28*, *D1Got209*, *D1Wox10*, *D1Rat169*, *D1Rat75*, *D1Rat77*, *D1Mit7*, *D1Rat119*, *D1Wox25*) was performed according to recommended conditions available in public rat databases. Direct DNA sequencing of the PCR-amplified products was performed as described [4].

2.3. Isolation of RNA, northern blot and microarray analyses, and real-time reverse-transcription PCR (RT-PCR)

Total RNA was extracted from tissues or cells using 1 ml of TRIzol reagent (Invitrogen). The purity and concentration of each RNA sample were determined by measuring the absorbance at 260/280 nm. To further determine the quality of RNA, 1 μg of total RNA was run on a 1% agarose gel to inspect the quality of the 28 S and 18 S ribosomal bands. cDNA was synthesised using a high capacity cDNA reverse transcription kit (Applied Biosystems) according to the manufacturer's instructions. A full-length cDNA probe for rat *Slc22a18* mRNA was prepared by cloning its RT-PCR product from rat liver into pGEM-T easy vectors (Promega) and its authenticity was confirmed by DNA sequencing. Total RNA (10 μg) was electrophoresed on a 1% agarose gel containing formaldehyde, and then transferred to a nylon membrane, Hybond N (Amersham Biosciences). Membranes were hybridised with [^{32}P] dCTP-labeled *Slc22a18* cDNA probes using a Megaprime DNA labeling kit in rapid-hyb buffer (Amersham Biosciences). After washing with 0.1× SSC, 0.1% SDS at 65 °C, the membranes were exposed to Kodak XAR-5 films (Kodak). Total RNA from rat epididymal adipose tissue was also subjected to an Oligotex mRNA purification kit (Takara Bio, Japan) and then analysed with a Rat Genome 230 2.0 Array (Affymetrix), which detected 20,861 rat genes expressed in adipose tissues. Gene expression was quantitatively analysed using real-time RT-PCR with LightCycler 480 SYBR Green I Master or LightCycler 480 Probes Master on a LightCycler 480 System II (Roche) as described previously [5]. DNA sequences of primers and probes that were used are listed in Supplementary Table 2. Messenger RNA of *36B4* was used as an RNA loading control for northern blot experiments and as an internal control in real-time RT-PCR.

2.4. Western blot analysis

A rabbit polyclonal antibody against rat Slc22a18 was generated by immunizing a rabbit with a synthetic peptide (C + KPLSQKGDKAR) for the C-terminal region of rat Slc22a18. Anti-mouse Slc22a18 antibody was also generated against a synthetic peptide (C + KPLSQKGEKAR) for its C-terminus. Anti V5-horseradish peroxidase (HRP)-conjugated antibody was obtained from Invitrogen, and antibodies against PPARγ and α-tubulin from Santa Cruz Biotechnology. Western blot analysis was performed as previously described [5] with some modifications. Whole cell lysates were prepared using lysis buffer (25 mM HEPES (pH7.9), 50 mM KCl, 6% glycerol, 5 mM EDTA, 5 mM $MgCl_2$, 1% TritonX100, 1 mM DTT, protease inhibitor cocktail (Roche)). Protein samples (50 μg) were subjected to 10% SDS–polyacrylamide gel electrophoresis (SDS–PAGE) or native–PAGE without SDS. Proteins were transferred to a polyvinylidene difluoride membrane (GE Healthcare), immunoblotted with appropriate antibodies, and visualised with an ImageQuant LAS 4000 mini (GE Healthcare).

2.5. Isolation of rat primary adipocytes and 3T3-L1 cell culture

Male rat epididymal fat pads were excised and minced in PBS with 0.5% BSA. Collagenase (Sigma–Aldrich) was added at 1 mg/ml before incubation at 37 °C for 2 h with shaking. Suspensions were centrifuged at 200*g* for 1 min to remove cellular debris and oil. Precipitated materials were resuspended as a vascular stromal fraction (VSF). Total RNA of floating adipocytes and the VSF were extracted separately with TRIzol reagent and subjected to RT-PCR. Mouse 3T3-L1 cells were maintained and differentiated in DMEM (WAKO, Japan) with 10% FBS as previously described [5]. On Day 0, 3T3-L1 preadipocytes were stimulated with a mixture comprising insulin, dexamethasone (DEXA) and 3-isobutyl-1-methylxanthine (IBMX) (all from Sigma), which induced the differentiation of preadipocytes into mature adipocytes. Oil Red O staining of 3T3-L1 cells was performed as previously described [5].

2.6. Adenoviral expression

Two independent constructs for short hairpin RNA (shRNA) targeting of *Slc22a18* were subcloned into the U6 entry vector using primer sequences specific for mouse *Slc22a18* cDNA (#1: 5′-gtgtaaccgttgacctgaaacgtgtgctgtccgtttcgggtcaatggttgcac-3′, #2: 5′-gggtcattatactcatctaacgtgtgctgtccgttaggtgagtatgatgatcc-3′) to generate adenoviral vectors by homologous recombination with the pAd promoterless vector (Invitrogen). Recombinant adenovirus was produced in 293A cells and purified as previously described [6]. The titer of adenovirus was determined using Adeno-X Rapid Titer kit (BD Biosciences). Four days before differentiation, 3T3-L1 cells were infected with adenoviral vectors for expressing shRNA (Ad-shSlc#1, Ad-shSlc#2, or Ad-shLacZ(control)) at the multiplicity of infection (MOI) of 30. Adenoviruses expressing GFP (Ad-GFP) or V5-tagged mouse Slc22a18 (Ad-Slc22a18V5) were also generated using the pAd/CMV/V5-DEST

vector system (Invitrogen) according to the manufacturer's instructions.

2.7. Data analysis and statistical analysis

Inter-strain differences were evaluated by the unpaired, two-tailed Student's *t* test. Comparison among three groups was performed using one-way ANOVA. *P*-values of <0.05 were considered significant. Logarithm of odds (LOD) scores in quantitative trait locus (QTL) analysis and marker locations were estimated using WinQTLCartographer ver.2.5 [7]. QTL plots were drawn based on the results of interval mapping analysis. The estimated threshold for a LOD score used as evidence of significant linkage in the F2 population was 2.4 (significance level = 0.05, permutation times = 1000).

3. Results

3.1. Decreased fat pad weight is linked to rat chromosome 1 (D1Rat240–D1Wox28) and not to Cd36

Initially, we examined for possible linkages between the mutant *Cd36* allele and each phenotype of the F2 population ($n = 144$) derived from a cross between the two different SHR strains. In this F2 cross, the mutant *Cd36* allele was significantly linked to altered metabolic phenotypes on the genetic background of these SHR strains. However, the difference in fat pad weight was not linked to the *Cd36* mutation, which indicated the possibility of another crucial mutation(s) underlying the differences in fat pad weight (Fig. 1A).

To explore this additional mutation, we continued our linkage analysis on this F2 population. The merit of this analysis was that it minimised the genetic noise derived from other genes, while a drawback was that there were few known genetic markers that could discriminate between these two SHR strains. After testing more than 500 candidate genetic markers selected from the public databases, we found 25 markers that could discriminate between them by agarose gel analysis or by SSCP analysis on polyacrylamide gels. In addition, 14 of these 25 polymorphic markers were located on rat chromosome 1 (Supplementary Table 3), which suggested that a different gross segment on rat chromosome 1 had possibly been separately inherited in these strains.

We then determined the genotypes using 11 markers located within about an 80 Mbp-segment flanked by *D1Wox32* and *D1Wox25* in all the F2 rats and performed a linkage analysis. These results showed significant linkage of the rat chromosome 1 region (*D1Rat240–D1Wox28*) with fat pad weight or fat pad weight adjusted for body weight with a maximum LOD score of 4.4 downstream of *D1Wox32* by 17.3 cM (Fig. 1B). It is worth noting that there was no linkage with body weight itself.

3.2. Identification of a splicing mutation in Slc22a18 at the linkage peak for reduced adiposity

We then compared the mRNA expression profiles in rat adipose tissues by microarray analysis. We selected genes that had considerable mRNA expression levels in adipose tissues or that had expression levels that were considerably different between the two SHR strains. By integrating both the positional and expression information, we focused on and comparatively sequenced 33 candidate genes (Supplementary Table 4). Among these, we found a biologically meaningful change only in the gene for solute carrier family 22 member 18 (Slc22a18). DNA sequence comparisons revealed that the SHR/NCrj strain, but not the SHR/Izm strain, had a G-to-A point mutation in the donor splice site of intron 9 (Fig. 2A). Northern blot analysis of mRNA derived from liver and kidney, two principal organs with *Slc22a18* mRNA expression, demonstrated slightly shorter bands in samples from strain SHR/NCrj as compared with those from strain SHR/Izm (Fig. 2B). RT-PCR analysis using primers located on exons 6 and 11 produced differentially-migrating bands (Fig. 2C). These were subjected to comparative DNA sequencing, which demonstrated that the mutation resulted in complete skipping of the whole exon 9 in the cDNA (Fig. 2D).

This skipping of exon 9 (102 bp) should have resulted in an in-frame deletion of 34 amino acids of rat Slc22a18 that comprises 412 amino acids [8] and is suggested to be a transporter with 10 membrane-spanning regions [9]. This in-frame deletion could cause a marked structural change, including a complete loss of the whole of the 8th membrane-spanning region. Western blot analysis confirmed these differentially-migrating bands at the protein level (Fig. 3A). Inclusion of this mutation increased the maximum LOD score up to 7.7 at the peak point downstream of *D1Wox32* by 17.3 cM, the exact location of the rat *Slc22a18* gene (Fig. 3B).

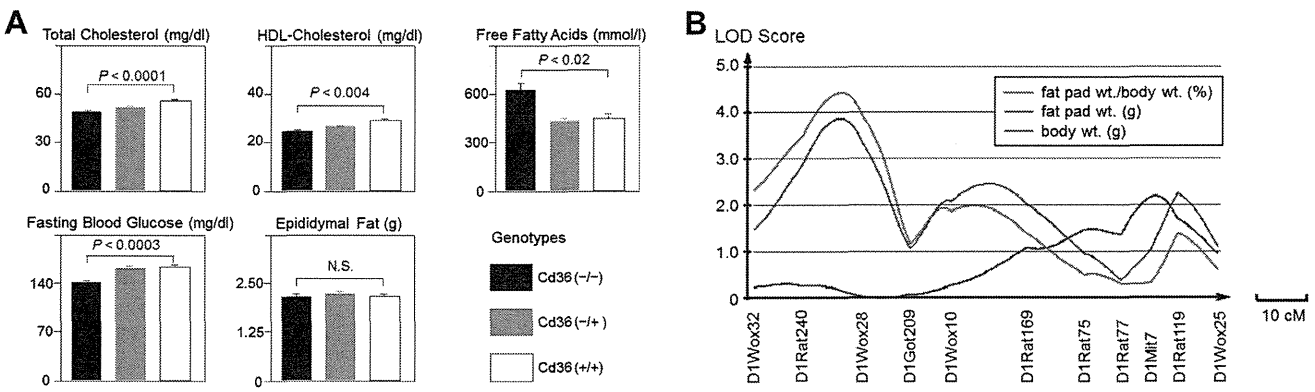

Fig. 1. Decreased epididymal fat pad weight is linked to a region on rat chromosome 1 and not to *Cd36*. (A) Linkage between the *Cd36* mutant allele and each phenotype was examined for F2 rats derived from a cross between strains SHR/NCrj and SHR/Izm (males, $n = 144$). Cd36(−/−) represents homozygous for the mutant *Cd36* allele, and Cd36(−/+) and Cd36(+/+) represent heterozygous and homozygous for the wild-type allele, respectively. (B) QTL plot for a gross segment of rat chromosome 1 (*D1Wox32–D1Wox25*) for epididymal fat pad weight (wt.), body wt., and epididymal fat pad wt. adjusted for (divided by) body wt. was made for the F2 population (SHR/NCrj × SHR/Izm) by determining the genotypes for 11 markers located within this segment. Significant linkage was observed between the rat chromosome 1 region (*D1Rat240–D1Wox28*) and fat pad wt. adjusted for body wt. with a maximum logarithm of odds (LOD) score of 4.4 at the point downstream of *D1Wox32* by 17.3 cM. Note that this linkage was independent of body wt.

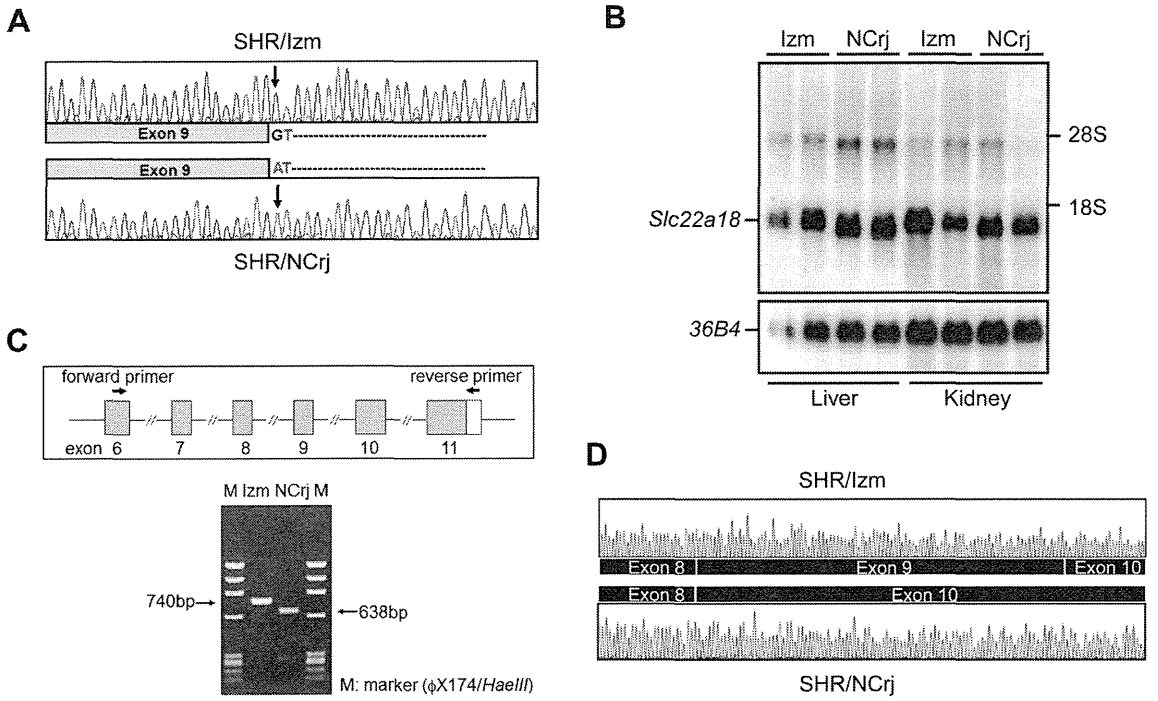

Fig. 2. Identification of a donor splice site mutation in the rat *Slc22a18* gene that results in exon skipping. (A) Comparative DNA sequencing of genomic DNA revealed a G-to-A point mutation in the donor splice site of intron 9 of the *Slc22a18* gene from strain SHR/NCrj with reduced adiposity. (B) Northern blot analysis of total RNA from the liver and kidney of each SHR using a probe for rat *Slc22a18* cDNA or *36B4*. (C) RT-PCR analysis of liver RNA with PCR-primers located on exons 6 and 11 produced differentially-migrating bands with agarose gel electrophoresis. (D) Comparative DNA sequencing of the RT-PCR products demonstrated a whole exon 9 deletion in the cDNA from strain SHR/NCrj, which was compatible with exon skipping because of the intron 9 donor splice site mutation.

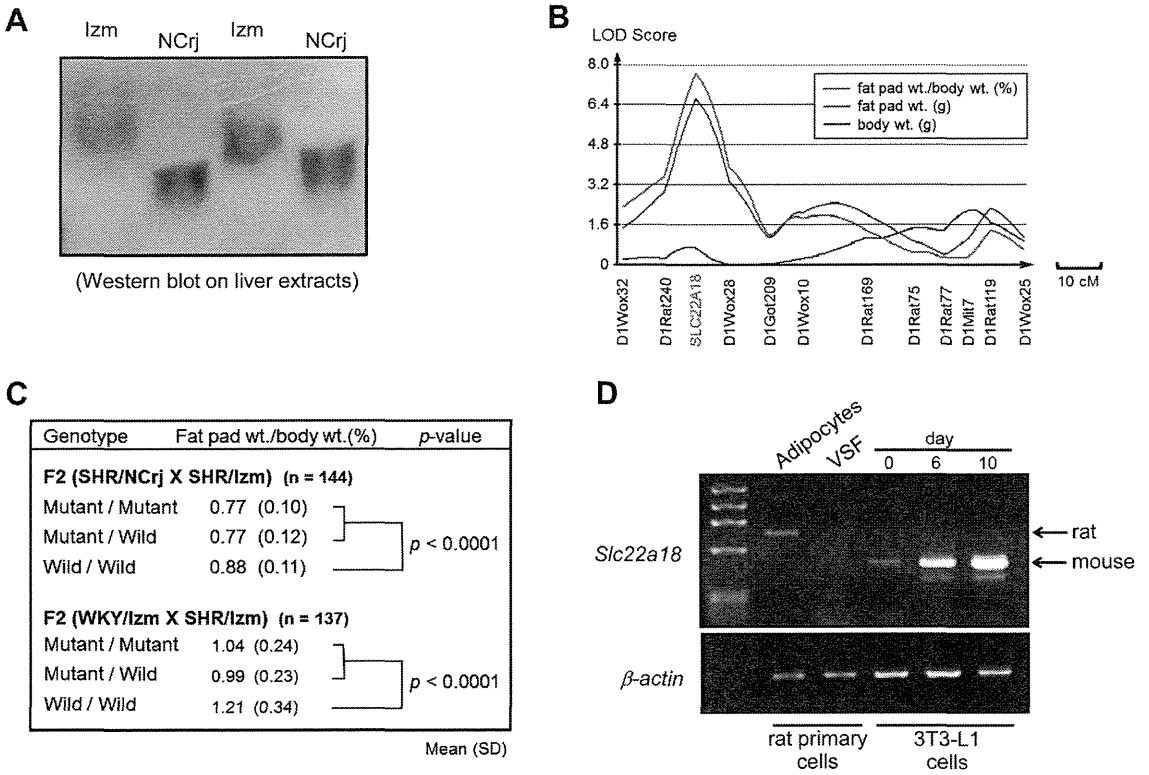

Fig. 3. Confirmation of the deletion at the protein level, localisation of the *Slc22a18* mutation at the linkage peak, replication of the linkage in another F2 cross, and *Slc22a18* mRNA expression relative to adipocyte differentiation. (A) Western blot analysis with a rabbit polyclonal antibody raised against a polypeptide of rat Slc22a18 showed differentially-migrating bands under non-denaturing conditions. (B) Including the mutation in the QTL analysis increased the maximum logarithm of odds (LOD) score up to 7.7 at the point where the rat *Slc22a18* gene is located. (C) Replication of significant linkage in two separate F2 crosses (SHR/NCrj × SHR/Izm and WKY/Izm × SHR/Izm). In both crosses, the mutant allele was significantly linked to reduced fat pad wt./body wt. in a quite similar dominant manner. (D) *Slc22a18* mRNA expression in differentiated adipocytes. RT-PCR results demonstrate that *Slc22a18* mRNA is expressed in isolated rat adipocytes rather than in the vascular stromal fraction (VSF). In 3T3-L1 cells, *Slc22a18* mRNA was abundantly expressed on Days 6 and 10 after stimulation with insulin + DEXA + IBMX in a differentiation-dependent manner.

3.3. Replication of linkage in another F2 cross

We examined the distribution of the *Slc22a18* mutation among the SHR-related strains. Unexpectedly, the mutant A-allele was prevalent among these rat strains including SHRSP or WKY rat, and the only exception was found in SHR/Izm sub-strains (Supplementary Fig. 1, Supplementary Table 1). Because all the other rat strains examined (e.g., Wistar/NCrj, Brown Norway, Sprague Dawley, Dahl/SS, Lewis) and all the reported sequences for other organisms always contained the wild-type allele, we postulated that this mutation may have originated from the ancestral Wistar colony from which both SHR and WKY were derived. This finding compelled us to make a comparison regarding the mutant *Slc22a18* allele in another F2 population derived from a cross between the SHR/Izm and WKY/Izm strains ($n = 137$). In this F2 comparison, a similar significant linkage was also observed in a similar dominant manner (Fig. 3C). This provided supporting evidence that the *Slc22a18* mutation itself or a mutation in a nearby gene should cause a decrease in adiposity independently of the genetic background.

3.4. Slc22a18 mRNA expression relative to adipocyte differentiation

Slc22a18 mRNA is ubiquitously expressed, although primarily in the liver and kidney [10]. We already observed considerable *Slc22a18* mRNA expression levels in rat adipose tissue by microarray analysis. Thus, we isolated rat primary adipocytes from a vascular stromal fraction (VSF) and examined *Slc22a18* mRNA expression by RT-PCR in these adipocytes and the VSF. These results showed that mRNA expression was mainly in isolated adipocytes but not in the VSF. Furthermore, in cultured 3T3-L1 cells, a model of preadipocyte to adipocyte differentiation [11], *Slc22a18* mRNA was expressed in a differentiation-dependent manner (Fig. 3D).

3.5. Knockdown and overexpression of Slc22a18 mRNA reciprocally regulates triglyceride accumulation and adipocyte differentiation in 3T3-L1 cells

To investigate the role of Slc22a18 in adipocyte differentiation, we examined the effects of knockdown of mouse *Slc22a18* mRNA on differentiation of 3T3-L1 cells. Adenoviral infection of either of the two independent shRNA constructs downregulated *Slc22a18* mRNA expression in 3T3-L1 cells up to less than 20% of the levels in control cells; the latter were infected with an adenoviral vector expressing *shLacZ* (Supplementary Fig. 2). On Day 8 after inducing differentiation, these control cells showed abundant lipid droplets (observed with Oil Red O staining) and massive protein expression for PPARγ and Slc22a18 (Fig. 4A). By contrast, a marked reduction in both lipid accumulation and PPARγ expression was observed in

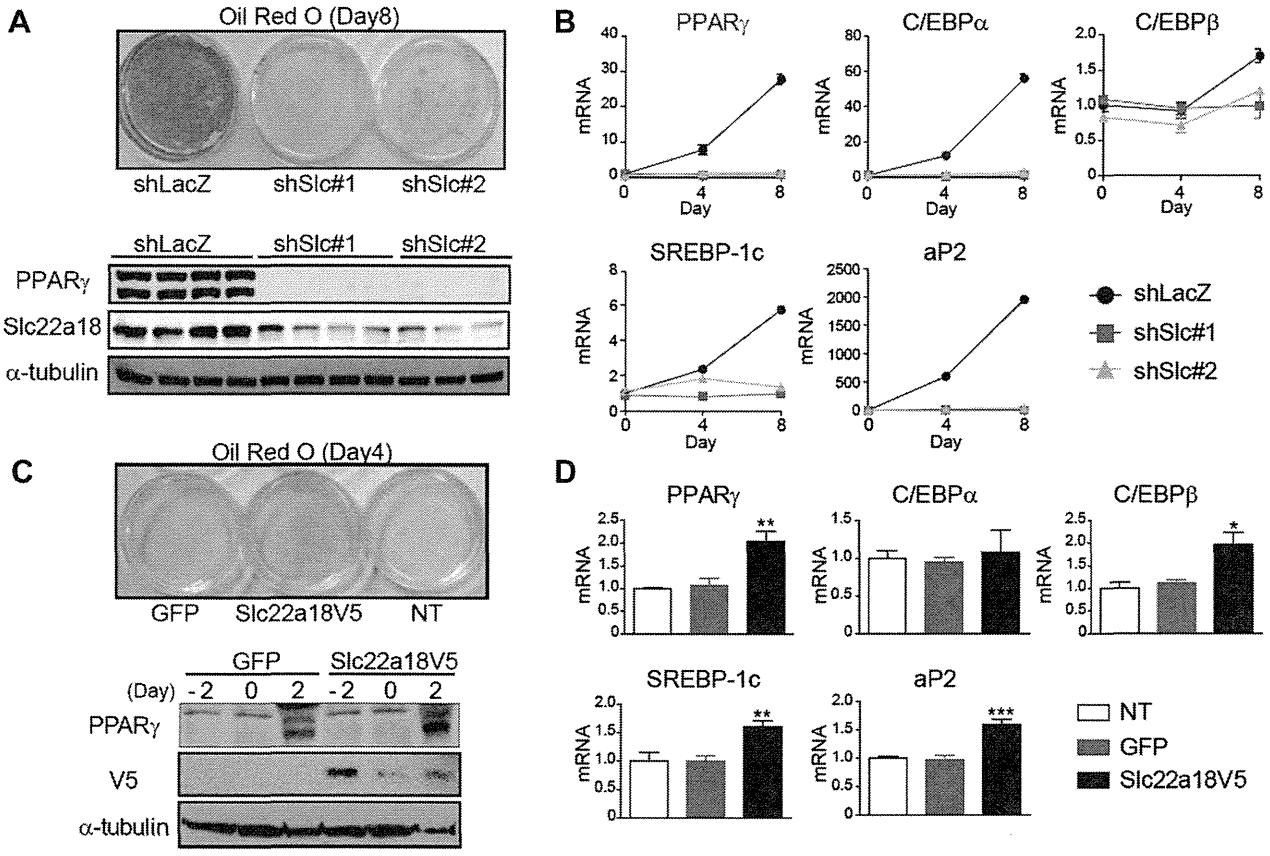

Fig. 4. The effects of knockdown and overexpression of *Slc22a18* on 3T3-L1 cell differentiation. (A) Top: triglyceride accumulation in 3T3-L1 cells on Day 8 was visualised using Oil Red O staining. Adenoviral vectors for expressing shRNA for *lacZ* or *Slc22a18* (shSlc#1 and shSlc#2) at an MOI of 30 were infected on Day −4. Bottom: western blot analysis of 3T3-L1 cells expressing each shRNA on Day 8. (B) The mRNA levels in 3T3-L1 cells expressing each shRNA on Day 0, 4, and 8 after inducing differentiation. Relative mRNA levels for adipogenic markers (PPARγ, C/EBPα, C/EBPβ, and SREBP-1c) and a mature adipocyte marker (aP2) were estimated after normalisation with 36B4. Results represent means ± SEM ($n = 3–4$ each). (C) Top: triglyceride accumulation in 3T3-L1 cells on Day 4 was detected using Oil Red O staining. The cells were infected with adenoviral vectors for expressing GFP or V5-tagged mouse Slc22a18 at an MOI of 140 or left without treatment (NT). Bottom: western blot analysis of 3T3-L1 cells expressing GFP or V5-tagged mouse Slc22a18 performed on Day −2, 0, and 2 after inducing differentiation. (D) Relative mRNA levels in each group of 3T3-L1 cells on Day 4 after inducing differentiation. Results represent means ± SEM ($n = 3–4$ each). Statistical significance in the comparison between GFP and Slc22a18V5 is shown as follows: $^{*}p < 0.05$, $^{**}p < 0.01$, $^{***}p < 0.001$.

the *Slc22a18*-knockdown cells. These phenotypic differences were consistent with the different mRNA expression profiles for adipocyte differentiation markers (PPARγ, C/EBPα, C/EBPβ, SREBP-1c, and aP2) whose mRNA expression levels increased progressively in the control cells but not in the *Slc22a18*-knockdown cells (Fig. 4B). On the other hand, overexpression of V5-tagged mouse Slc22a18 promoted lipid accumulation and protein expression for PPARγ (Fig. 4C) and increased mRNA expression for several adipocyte differentiation markers in mature 3T3-L1 cells on Day 4 after inducing differentiation (Fig. 4D). These results suggest that *Slc22a18* plays an important role in triglyceride accumulation and is involved in the induction of regulatory genes necessary for adipocyte differentiation.

4. Discussion

We previously reported a crucial genetic difference (*Cd36* mutation) between the SHR/NCrj and SHR/Izm strains [2]. In this study, we found a gross genome segment on rat chromosome 1 that was quite different between these SHR strains and found a significant linkage of this region to altered adiposity in the SHR. We identified a splicing mutation in the rat *Slc22a18* gene located exactly at the peak of this linkage. The mutant allele was prevalent among as well as restricted to SHR-related strains, which provides new insights into the ancestral Wistar colony from which the SHR was derived.

The SLC (solute carrier) family comprises a large number of transporters. To date, a total of 52 subfamilies and nearly 400 different genes have been identified [12]. Evidence has recently been accumulating that gene mutations in these SLC family members underlie a variety of human diseases [13,14]. However, with regard to SLC22A18 (also known as BWSCR1A, BWR1A, IMPT1, ORCTL2, and TSSC5), only a small number of papers have been published so far. Although several reports have suggested its possible association with cancer development or progression [15,16], the physiological role of SLC22A18 remains largely unknown. In this study, we found a tight linkage between *Slc22a18* mutation and reduced fat pad weight in two separate F2 comparisons. Furthermore, a significant linkage was restricted to fat pad weight or fat pad weight/body weight, but was not observed with body weight. These data seem compatible with the hypothesis that *Slc22a18* plays a role in local fat accumulation within adipose tissues. Our results demonstrating considerable *Slc22a18* mRNA expression levels in primary adipocytes and its differentiation-dependent expression, at least in 3T3-L1 cells, support the aforementioned hypothesis. More convincing evidence comes from our results demonstrating a close relationship between *Slc22a18* mRNA expression and adipocyte differentiation in cultured 3T3-L1 cells. Together, these results suggest that *Slc22a18* regulates fat accumulation *in vitro* and *in vivo*. Although further research is needed to elucidate the physiological function of Slc22a18, manipulating its function, if possible, may constitute a novel therapeutic target in obesity.

Acknowledgments

This study was supported in part by Grants-in Aid for Scientific Research from the Ministry of Education, Culture, Sports, Science and Technology in Japan (to T.Y. Y.I. and T.G.) and by Grants-in-Aid for Intractable Diseases from the Ministry of Health, Labour and Welfare of Japan (to T.G.)

Appendix A. Supplementary data

Supplementary data associated with this article can be found, in the online version, at http://dx.doi.org/10.1016/j.bbrc.2013.09.096.

References

[1] G.M. Reaven, H. Chang, Relationship between blood pressure, plasma insulin and triglyceride concentration, and insulin action in spontaneous hypertensive and Wistar-Kyoto rats, Am. J. Hypertens. 4 (1 PT 1) (1991) 34–38.
[2] T. Gotoda, Y. Iizuka, N. Kato, J. Osuga, M.T. Bihoreau, T. Murakami, Y. Yamori, H. Shimano, S. Ishibashi, N. Yamada, Absence of Cd36 mutation in the original spontaneously hypertensive rats with insulin resistance, Nat. Genet. 22 (1999) 226–228.
[3] M. Febbraio, E. Guy, C. Coburn, F.F. Knapp Jr., A.L. Beets, N.A. Abumrad, R.L. Silverstein, The impact of overexpression and deficiency of fatty acid translocase (FAT)/CD36, Mol. Cell. Biochem. 239 (2002) 193–197.
[4] T. Gotoda, B.S. Manning, A.P. Goldstone, H. Imrie, A.L. Evans, A.D. Strosberg, P.M. McKeigue, J. Scott, T.J. Aitman, Leptin receptor gene variation and obesity: lack of association in a white British male population, Hum. Mol. Genet. 6 (1997) 869–876.
[5] N. Inoue, N. Yahagi, T. Yamamoto, M. Ishikawa, K. Watanabe, T. Matsuzaka, Y. Nakagawa, Y. Takeuchi, K. Kobayashi, A. Takahashi, H. Suzuki, A.H. Hasty, H. Toyoshima, N. Yamada, H. Shimano, Cyclin-dependent kinase inhibitor, p21WAF1/CIP1, is involved in adipocyte differentiation and hypertrophy, linking to obesity, and insulin resistance, J. Biol. Chem. 283 (2008) 21220–21229.
[6] T. Yamamoto, K. Watanabe, N. Inoue, Y. Nakagawa, N. Ishigaki, T. Matsuzaka, Y. Takeuchi, K. Kobayashi, S. Yatoh, A. Takahashi, H. Suzuki, N. Yahagi, T. Gotoda, N. Yamada, H. Shimano, Protein kinase Cbeta mediates hepatic induction of sterol-regulatory element binding protein-1c by insulin, J. Lipid Res. 51 (2010) 1859–1870.
[7] S. Wang, C.J. Basten, Z.-B. Zeng, Windows QTL Cartographer 2.5. Department of Statistics, North Carolina State University, Raleigh, NC, (http://statgen.ncsu.edu/qtlcart/WQTLCart.htm) 2012.
[8] E.G. Tzortzaki, M. Yang, D. Glass, L. Deng, A.P. Evan, S.B. Bledsoe, P.J. Stambrook, A. Sahota, J.A. Tischfield, Impaired expression of an organic cation transporter, IMPT1, in a knockout mouse model for kidney stone disease, Urol. Res. 31 (2003) 257–261.
[9] H.Y. Yamada, G.J. Gorbsky, Tumor suppressor candidate TSSC5 is regulated by UbcH6 and a novel ubiquitin ligase RING105, Oncogene 25 (2006) 1330–1339.
[10] D. Dao, D. Frank, N. Qian, D. O'Keefe, R.J. Vosatka, C.P. Walsh, B. Tycko, IMPT1, an imprinted gene similar to polyspecific transporter and multi-drug resistance genes, Hum. Mol. Genet. 7 (1998) 597–608.
[11] C.S. Rubin, A. Hirsch, C. Fung, O.M. Rosen, Development of hormone receptors and hormonal responsiveness *in vitro*. Insulin receptors and insulin sensitivity in the preadipocyte and adipocyte forms of 3T3-L1 cells, J. Biol. Chem. 253 (1978) 7570–7578.
[12] http://www.bioparadigms.org/slc/intro.htm.
[13] A. Enomoto, H. Kimura, A. Chairoungdua, Y. Shigeta, P. Jutabha, S.H. Cha, M. Hosoyamada, M. Takeda, T. Sekine, T. Igarashi, H. Matsuo, Y. Kikuchi, T. Oda, K. Ichida, T. Hosoya, K. Shimokata, T. Niwa, Y. Kanai, H. Endou, Molecular identification of a renal urate anion exchanger that regulates blood urate levels, Nature 417 (2002) 447–452.
[14] R. Yamada, S. Tokuhiro, X. Chang, K. Yamamoto, SLC22A4 and RUNX1: identification of RA susceptible genes, J. Mol. Med. (Berl.) 82 (2004) 558–564.
[15] C. Schwienbacher, S. Sabbioni, M. Campi, A. Veronese, G. Bernardi, A. Menegatti, I. Hatada, T. Mukai, H. Ohashi, G. Barbanti-Brodano, C.M. Croce, M. Negrini, Transcriptional map of 170-kb region at chromosome 11p15.5: identification and mutational analysis of the BWR1A gene reveals the presence of mutations in tumor samples, Proc. Natl. Acad. Sci. USA 95 (1998) 3873–3878.
[16] S.H. Chu, Y.B. Ma, D.F. Feng, H. Zhang, Z.A. Zhu, Z.Q. Li, P.C. Jiang, Correlation of low SLC22A18 expression with poor prognosis in patients with glioma, J. Clin. Neurosci. 19 (2012) 95–98.

Original Article

Apolipoprotein C-II Deficiency with No Rare Variant in the *APOC2* Gene

Satoru Takase[1], Jun-ichi Osuga[2], Hayato Fujita[1], Kazuo Hara[1], Motohiro Sekiya[1], Masaki Igarashi[1], Mikio Takanashi[1], Yoshinori Takeuchi[1], Yoshihiko Izumida[1], Keisuke Ohta[1], Masayoshi Kumagai[1], Makiko Nishi[1], Midori Kubota[1], Yukari Masuda[1], Yoshino Taira[1], Sachiko Okazaki[1], Yoko Iizuka[1], Naoya Yahagi[1], Ken Ohashi[1], Hiroshi Yoshida[3], Hidekatsu Yanai[4], Norio Tada[4], Takanari Gotoda[5], Shun Ishibashi[2], Takashi Kadowaki[1] and Hiroaki Okazaki[1,6]

[1]Department of Diabetes and Metabolic Diseases, Graduate School of Medicine, The University of Tokyo, Tokyo, Japan
[2]Division of Endocrinology and Metabolism, Department of Medicine, Jichi Medical University, Tochigi, Japan
[3]Department of Laboratory Medicine, Jikei University Kashiwa Hospital, Chiba, Japan
[4]Division of General Medicine, Jikei University Kashiwa Hospital, Chiba, Japan
[5]Department of Clinical and Molecular Epidemiology, 22nd Century Medical and Research Center, University of Tokyo Hospital, Tokyo, Japan
[6]Molecular Medicinal Sciences on Metabolic Regulation, Graduate School of Medicine, The University of Tokyo, Tokyo, Japan

Aim: **Familial apolipoprotein C-II (apoC-II) deficiency is a rare autosomal recessive disorder with marked hypertriglyceridemia resulting from impaired activation of lipoprotein lipase. In most cases of apoC-II deficiency, causative mutations have been found in the protein-coding region of *APOC2*; however, several atypical cases of apoC-II deficiency were reported to have markedly reduced, but detectable levels of plasma apoC-II protein (hereafter referred to as hypoapoC-II), which resulted from decreased promoter activity or improper splicing of apoC-II mRNA due to homozygous mutations in *APOC2*. Here we aim to dissect the molecular bases of a new case of hypoapoC-II.**

Methods: **We performed detailed biochemical/genetic analyses of our new case of hypoapoC-II, manifesting severe hypertriglyceridemia (plasma triglycerides, 3235 mg·dL^{-1}) with markedly reduced levels of plasma apoC-II (0.6 mg·dL^{-1}).**

Results: **We took advantage of a monocyte/macrophage culture system to prove that transcription of apoC-II mRNA was decreased in the patient's cells, which is compatible with the reported features of hypoapoC-II. Concomitantly, transcriptional activity of the minigene reporter construct of the patient's *APOC2* gene was decreased; however, no rare variant was detected in the patient's *APOC2* gene. Fifty single nucleotide variants were detected in the patient's *APOC2*, but all were common variants (allele frequencies >35%) that are supposedly not causative.**

Conclusions: **A case of apoC-II deficiency was found that is phenotypically identical to hypoapoC-II but with no causative mutations in *APOC2*, implying that other genes regulate apoC-II levels. The clinical entity of hypoapoC-II is discussed.**

J Atheroscler Thromb, 2013; 20:481-493.

Key words; Chylomicronemia, Apolipoprotein C-II deficiency, Single nucleotide polymorphism, *cis*-regulatory region, Rare variant

Address for correspondence: Hiroaki Okazaki, Department of Diabetes and Metabolic Diseases, Graduate School of Medicine, The University of Tokyo, 7-3-1 Hongo, Bunkyo-ku, Tokyo 113-8655, Japan
E-mail: hokazaki-tky@umin.ac.jp
Received: November 6, 2012
Accepted for publication: December 7, 2012

Introduction

Hypertriglyceridemia is of clinical importance not only as a sign of metabolic syndrome, but also as an independent risk factor for cardiovascular events[1-3]. Elucidation of the mechanisms of hypertriglyceridemia is an emerging need with the worldwide preva-

lence of metabolic syndrome. Triglycerides (TG) are carried in the form of TG-rich lipoproteins (TGRL) in plasma. TGRLs are secreted either as chylomicrons from the intestine or as very low density lipoproteins (VLDL) from the liver, followed by catabolism by lipoprotein lipase (LPL) that hydrolyzes TGs in TGRL with subsequent uptake of remnant lipoproteins primarily by the liver. A defect in one of these pathways results in hypertriglyceridemia[4].

ApoC-II, a member of the apoE/apoC-I/apoC-IV/apoC-II gene cluster, is a 79-amino-acid polypeptide primarily biosynthesized in the liver and intestine, and is present on plasma chylomicrons, VLDL, and high-density lipoproteins (HDL). ApoC-II plays an important role as a co-factor of LPL[5, 6]. The importance of apoC-II in regulating plasma TG levels is evidenced by human apoC-II deficiency[7], which is a rare autosomal recessive disorder characterized by extreme hypertriglyceridemia, as seen in LPL deficiency[8, 9].

The molecular defects of apoC-II deficiency are heterogeneous. Most cases had causative mutations in the protein-coding region of the apoC-II gene (*APOC2*)[10], resulting in null apoC-II (an initiation codon mutation[11]), or nonfunctional apoC-II protein (nonsense mutations[12]; frameshift mutations[13]; missense mutations[14] (reviewed in[15, 16])). Notably, several cases were reported to have markedly reduced, but detectable levels of apoC-II protein with apparently normal electrophoretic patterns (for simplicity, hereafter referred to as hypoapoC-II)[17-19]. These are all characterized by a reduction in apoC-II mRNA transcription due to i) decreased promoter activity of *APOC2* (apoC-II$_{Köln}$[19]), or ii) a donor splice-site mutation of intron 2 of *APOC2* that results in markedly reduced levels of apoC-II mRNA (ApoC-II$_{Hamburg}$[17], ApoC-II$_{Tokyo}$[18]).

We report a patient with apoC-II deficiency in which no causative mutations were detected in the apoC-II gene. Our patient is a typical case of hypoapoC-II manifesting hypertriglyceridemia, coincided with markedly reduced, but detectable levels of apoC-II in plasma. As in other reported cases of hypoapoC-II, apoC-II mRNA transcription was decreased by 50%, at least partially due to reduced transcriptional activity of the *cis*-regulatory region of the patient's *APOC2* gene, as shown by minigene reporter experiments. However, no rare variant was identified in any regions of *APOC2*, suggesting the involvement of additional genetic defect(s) that regulate apoC-II protein levels in plasma. To our knowledge, this is the first report of apoC-II deficiency with no rare variant found in the *APOC2* gene. Together with other cases[17-19], the clinical entity of hypoapoC-II is discussed.

Table 1. Biochemical characteristics of the patient at the time of presentation

Total cholesterol ($mg \cdot dL^{-1}$)	249
HDL-cholesterol ($mg \cdot dL^{-1}$)	39.8
Triglycerides ($mg \cdot dL^{-1}$)	1435
Apolipoprotein A-I ($mg \cdot dL^{-1}$)	120
Apolipoprotein A-II ($mg \cdot dL^{-1}$)	28.3
Apolipoprotein B ($mg \cdot dL^{-1}$)	121
Apolipoprotein C-II ($mg \cdot dL^{-1}$)	ND
Apolipoprotein C-III ($mg \cdot dL^{-1}$)	28.0
Apolipoprotein E ($mg \cdot dL^{-1}$)	19.9
Apolipoprotein E genotype	E3/E3

At the time of evaluation of these laboratory data, the patient was treated with fenofibrate (600 mg per day) and ethyl icosapentate (1800 mg per day). Apolipoprotein E genotype was determined by restriction fragment length polymorphism analysis using PCR primers (5'-TCCAAGGAGCTGCAGGCGGCGCA-3' and 5'- GCCCCGGCCTGGTACACTGCCA-3') and restriction endonucleases (AflIII and HaeII) as described previously (Zivelin A et al. Clin Chem 1997; 43: 1657-1659). ND: not detected.

Methods

Subjects

The proband was a 47-year-old Japanese man manifesting type I hyperlipidemia (plasma level of triglycerides, 3235 $mg \cdot dL^{-1}$; total cholesterol, 385 $mg \cdot dL^{-1}$) with recurrent episodes of pancreatitis. This patient was previously characterized and reported as having apoC-II deficiency[20]. The diagnosis of apoC-II deficiency was made based on undetectable levels of apoC-II protein by the immunodiffusion assay. On referral to our hospital, he had been treated with fenofibrate and ethyl icosapentate. He also had a past medical history of conversion disorder with several episodes of cataplexy starting at age 36 years. Detailed clinical characteristics are available in **Table 1** as well as in the previous report[20].

In addition to the proband, his normolipidemic parent (mother) was investigated. Unrelated control subjects without hypertriglyceridemia were also investigated. His father's biological sample was unavailable since he had died at age 42 years with the diagnosis of cerebral vascular disease. Although his parents were not related, we found a case of consanguinity in his family (the patient's uncle and aunt were related), and consanguinity was rather common in the local community where both of his parents were raised.

Informed consent was obtained from the subjects, and all procedures were subjected to approval by the human genome, gene analysis research ethics committee of the University of Tokyo.

Table 2. Sequences of PCR primers for cloning human cDNA probes

cDNA probe	Sequences of forward and reverse primers	PCR product *bp*
apoC-II	5'-AGGACAGCCTGCCAGAGTCTG-3'	462
	5'-AGAATTCAGGCTAGAGTTGGGAG-3'	
apoC-IV	5'-AGAAATGTCCCTCCTCAGAAACAG-3'	393
	5'-AACATTTTAACCCTGGTCCTTGTC-3'	
CLPTM1	5'-CATGTGTACATCTCAGAGCACG-3'	566
	5'-GATGGGGTAGTAGTCCTTCTGC-3'	
MCSF	5'-TCGGAGTACTGTAGCCACATGA-3'	638
	5'-ACTGCCTGGATCCACTGTGT-3'	

Biochemical Analyses of Plasma Apolipoproteins

Blood was obtained from the patient, his mother, and normal control subjects. Fractions of plasma, buffy coat and total blood cells were separated by low-speed centrifugation. The buffy coat was stored at −80℃ until processed later to obtain genomic DNA as described in the following section. One microliter of plasma was subjected to sodium dodecyl sulfate polyacrylamide gel electrophoresis (SDS-PAGE), and immunoblot analysis using anti-human apoC-II polyclonal antibody (Calbiochem, San Diego, CA, USA). Apolipoprotein control serum- Daiichi High (Daiichi Pure Chemicals Co., Ltd., Tokyo, Japan), was used as a standard to assess plasma concentrations of apoC-II.

For isoelectric focusing (IEF) of plasma apolipoproteins, TGRLs, isolated by ultracentrifugation, were delipidated with ethanol:diethylether (3:1) to obtain apolipoproteins, which were then subjected to electrophoresis using Immobiline DryStrip (pH 4-7; GE Healthcare, Tokyo, Japan) according to the manufacturer's instructions; proteins were visualized by Coomassie brilliant blue staining. For two-dimensional PAGE (2D-PAGE), TGRL apolipoproteins were separated by IEF, then by SDS-PAGE, and apoC-II protein was detected by immunoblotting using the same anti-apoC-II antibody as described above.

Lipase Activity Assay

Post-heparin plasma (PHP) was obtained 15 min after an intravenous injection of heparin (30 units·kg^{-1}) to overnight fasted subjects. Lipase activity in plasma (6.7 μL/reaction) was determined by measuring the amount of FFA released from ^{3}H-triolein emulsions (Amersham Biosciences, Tokyo, Japan) as described previously[21, 22], and expressed as $\mu mol^{-1} \cdot h^{-1} \cdot mL^{-1}$. LPL activity was calculated by subtracting the activity in the presence of 1 mol·L^{-1} NaCl (representing hepatic triglyceride lipase (HTGL) activity) from the activity in the absence of 1 mol·L^{-1} NaCl (total lipase activity). Various amounts of plasma from normolipidemic subjects were added to the assay mixture to supply an excess amount of apoC-II proteins.

Northern Blot Analysis of Primary Monocytes/ Macrophages Derived from Peripheral Blood

Human monocytes/macrophages were isolated from peripheral blood by Lymphoprep (Nycomed, Roskiled, Denmark), and cultured as described previously[23]. On day 7, cells were incubated with or without 10 μmol·L^{-1} of Liver X receptor (LXR) agonist (T0901317) for 24 h, and harvested. In a separate experiment, actinomycin D (Sigma-Aldrich, Tokyo, Japan) was added to the incubation medium at 10 μg·L^{-1} to inhibit RNA synthesis.

Total RNA was isolated from cells by TRIzol reagent (Invitrogen Corp., Tokyo, Japan), and equal amounts of RNA were subjected to Northern blot analysis as described[23]. Probes for apoC-II, apoC-IV, cleft lip and palate associated transmembrane protein 1 (CLPTM1), and monocyte colony stimulating factor (MCSF) were constructed from cDNA fragments amplified by RT-PCR using cDNA obtained from monocytes/macrophages as a template. Probes for apoE and ribosomal protein, large, P0 (RPLP0) were previously described[23, 24]. Primer sequences used for each probe construction are listed in **Table 2**. Signals were detected and analyzed by Phosphor-Imager Screen and BASTATION software (FUJIFILM Corp., Tokyo, Japan). Intensity of each band was measured by ImageJ 1.39 software (NIH).

Southern Blot Analysis and Genomic DNA Copy Number Analysis

Genomic DNA (10 μg/reaction) were digested with 5 units of XbaI, SacI, PstI, EcoRI and BamHI (New England Biolabs, Beverly, MA, USA) at 37℃

Table 3. Sequences of PCR primers for DNA copy number analysis

Target gene	Sequences of forward and reverse primers	PCR product *bp*
APOC2	5'-GGGCTCTCCTGACACACTCT-3'	243
	5'-TGGATGCAGTCGGTGGTAT-3'	
RPLP0	5'-GCTCCTCTTAGGCCCGGGAC-3'	185
	5'-ACCCTGCACTTACGATGATCTTAAGGA-3'	

overnight, and subjected to Southern blot analysis as described previously[22].

For DNA copy number analysis, genomic DNA (25 ng/reaction) was subjected to real-time PCR by LightCycler 480 system II (Roche Applied Science, Tokyo, Japan) to amplify the *APOC2* gene and *RPLP0* gene (as a control). Primer pairs (**Table 3**) were designed to amplify genomic DNA, but not mRNA. Cycle numbers for a given threshold were determined for both *APOC2* and *RPLP0*, and the relative DNA copy number (*APOC2*/*RPLP0*) was calculated.

Sequencing the *APOC2* and Other Genes in Plasma TG Metabolism

Genomic DNA was extracted from the buffy coat obtained from peripheral blood as described above, using the Blood & Cell Culture DNA Mini Kit (Qiagen GmbH, Hilden, Germany) according to the manufacturer's instructions. The *APOC2* gene, spanning from the 3' end of the last exon of the *APOC4* to the 5' end of the first exon of *CLPTM1*, was amplified by PCR using genomic DNA (0.1 μg/reaction), PrimeSTAR GXL DNA polymerase (Takara Bio Inc., Otsu, Japan), and a set of primer pairs as listed in **Table 4**. The PCR condition was as follows: 30 cycles of denaturation (98℃ for 10s) and extension (68℃ for 1 min/kb). The PCR fragment was purified by the MinElute Gel Extraction Kit (Qiagen), and sequenced using DNA sequencer CEQ 2000 (Beckman Coulter, Inc., Tokyo, Japan) with primers described in **Table 5**. Alternatively, 3 to 7 subclones were sequenced to compensate for possible errors during extension with GXL polymerase. Other genes involved in plasma TG metabolism (*LPL*, apolipoprotein A-V (*APOA5*), apolipoprotein C-III (*APOC3*), lipase maturation factor 1 (*LMF1*), GPI-anchored high-density lipoprotein (HDL)-binding protein 1 (*GPIHBP1*)) were sequenced as described[25, 26].

Dual Luciferase Reporter Gene Assays

Reporter constructs containing the *APOC2* minigene were constructed as follows: The PCR product of the *APOC2* gene as described above was cloned into pGEM-T Easy vector (Promega Corporation, Madison, WI, USA) using the In-Fusion PCR Cloning Kit (Clontech Laboratories, Inc., Mountain View, CA, USA); thereafter, the firefly luciferase gene was inserted just before the apoC-II stop codon to generate an *APOC2* minigene reporter construct. HEK293 cells and HepG2 cells were plated in a 48-well plate in triplicate, followed by transient transfection with 300 ng of the reporter construct along with 20 ng Renilla expression vector (pRL-SV40 (Promega), as a transfection control) using Attractene transfection reagent (Qiagen). Cells were lysed 48 h after transfection and cell lysates were used for the measurement of firefly and Renilla luciferase activities according to the supplier's instructions (Promega for firefly luciferase; Toyo B-Net Co., Ltd (Tokyo, Japan) for Renilla luciferase). The firefly luciferase activities were normalized against control Renilla luciferase activities.

Table 4. Sequences of PCR primers for DNA amplification of the *APOC2* gene

Direction	Primer sequences
forward	5'-TCTAGAGGATCCTTCCCCAGTGTGGC-3'
reverse	5'-AGGACAAGACTCTCAGAGGCT-3'

Genotyping of Single Nucleotide Polymorphisms (SNPs) in *APOC2*

We included 384 persons who participated in an annual health check conducted by the Hiroshima Atomic Bomb Casualty Council Health Management Center (Hiroshima, Japan). Written informed consent was obtained from all the participants. We genotyped variants by direct sequencing, performed with the BigDye terminator (Life Technologies, Carlsbad, CA) and resolved by an ABI 3700 automated DNA sequencer (Life Technologies). The results were integrated using a Sequencher (Gene Codes, Ann Arbor, MI). Variants were genotyped manually.

Table 5. Primers for sequencing the *APOC2* gene and the intergenic region between *APOC2* and *CLPTM1*

Position in gene	Direction	Primer sequences
Promoter, Exon 1	fw	5'-AAGCTCTGACTCCATTCCCA-3'
Promoter, Exon 1	rv	5'-ACACGGGCTTCTAATA-3'
Intron 1	fw	5'-CGGAGCTGGTGAGGACA-3'
Intron 1	fw	5'-TGAGCTTCTGCTTAGAGTTAGGGT-3'
Intron 1	rv	5'-CACCTCAGCCACCCTAACTCTA-3'
Intron 1	fw	5'-AACTGTAGGCTGGGCGTG-3'
Intron 1	fw	5'-AATTGTAGACCATTTGCTTGTGTTC-3'
Intron 1	fw	5'-ATTAGCAGCTGGGCATGGT-3'
Intron 1, Exon 2	rv	5'-TGGGCTGGGAAGATGCT-3'
Exon 2, Intron 2	fw	5'-GCTGTGTCCAAGTCCATGC-3'
Intron 2, Exon 3	rv	5'-TGGATGCAGTCGGTGGTAT-3'
Exon 3, Intron 3	fw	5'-GGGCTCTCCTGACACACTCT-3'
Exon 4	fw	5'-CTCCCTCTAACCATCTGTGCTT-3'
Exon 4	rv	5'-GCTGAGGCACACAGAATCG-3'
Intergenic region	fw	5'-CAATCTCGGCTCACTGC-3'
Intergenic region	fw	5'-CATAGACACAGCTAGTCCACAGTG-3'
Intergenic region	fw	5'-CCTAGGCTAGTCTCCAATTCCTG-3'
Intergenic region	fw	5'-GCCAAGATTCCTGTATCCTGAG-3'
Intergenic region	fw	5'-GTGGGGAGGGGAAGACCCTG-3'
Intergenic region	fw	5'-TCAGAGTAGCTGGACCACAGG-3'
Intergenic region	fw	5'-AGTGCGATGGCATGATCT-3'
Intergenic region	fw	5'-GAATTCAGTGGCATGATCTT-3'
Intergenic region	rv	5'-GTCTGTAACTCCAGCTACTCG-3'
Intergenic region	fw	5'-ATACAGCAGTGACCACAACA-3'
Intergenic region	rv	5'-TGTTGTGGTCACTGCTGTAT-3'
Intergenic region	fw	5'-CCATCTAACTACGTCTTCCCA-3'

fw, forward; rv, reverse.

Statistical Analyses

Results are presented as the means ± SE. Student's *t*-test was employed to compare the means between two groups. All calculations were performed with Stat View version 5.0 for Windows (SAS Institute Japan Ltd., Tokyo, Japan).

Results

Electrophoretic Analysis of Plasma ApoC-II Protein

First, we performed immunoblot analysis of the patient's serum using anti-human apoC-II polyclonal antibody to assess if the patient's serum was deficient in apoC-II even with this highly sensitive method. Unexpectedly, a trace amount of apoC-II protein was identified in the patient's plasma (**Fig. 1A**). The concentration of apoC-II in the patient's plasma was estimated to be 0.6 $mg \cdot dL^{-1}$, which was well below the average plasma apoC-II concentration of healthy Japanese subjects (2.9 ± 1.3 $mg \cdot dL^{-1}$)[27], and that of heterozygotic cases of apoC-II deficiency (1.8 ± 0.5 $mg \cdot dL^{-1}$)[28]. Notably, the molecular weight of the patient's apoC-II was identical to that of the normal subject. The electrophoretic patterns of the patient's residual apoC-II were also indistinguishable from that of the normal subject as demonstrated by IEF (**Fig. 1B**) or by 2D-PAGE (**Fig. 1C**), suggesting that the patient's plasma contains apoC-II protein, albeit at markedly reduced levels. These phenotypes are compatible with those of the reported cases of hypoapoC-II[17-19].

Lipoprotein Lipase Activity in Post-Heparin Plasma (PHP)

Next, we assessed if LPL activity was impaired in the patient's plasma. Without the addition of normal plasma, LPL activity of the patient's PHP was reduced by 48% compared with that of the control subject (control vs. the patient: 8.6 vs. 4.5 $\mu mol \cdot h^{-1} \cdot mL^{-1}$). Addition of normal plasma dose-dependently increased the patient's LPL activity by 1.5-fold (4.5,

5.8, and 6.6 μmol·h^{-1}·mL^{-1}, by the addition of 0, 0.5, and 1 μL of normal plasma, respectively), indicating that the patient's plasma lacked a co-factor for LPL, but not LPL *per se*. HTGL activity was found to be reduced in the patient's PHP (control vs. the patient: 10.3 vs. 2.4 μmol·h^{-1}·mL^{-1}), as often seen in homozygous apoC-II deficiency for unknown reasons[6].

Northern Blot Analysis of Primary Monocytes/ Macrophages Derived from Peripheral Blood

One possible explanation for the decreased levels of plasma apoC-II protein might be some defects in apoC-II mRNA transcription, as reported in other cases of hypoapoC-II. To rule out this possibility, we first measured mRNA levels of apoC-II in monocytes/ macrophages isolated from peripheral blood, known cell types that express apoC-II endogenously[29]. With only 2 μg of total RNA loaded, we successfully detected abundant mRNA expression of apoC-II in the monocytes/macrophages of normal control subjects (**Fig. 2A**). In contrast, the patient's monocytes/macrophages showed 60% reduction in apoC-II mRNA compared with normal control subjects, whereas the mRNA levels remained unchanged for all other genes tested: apoC-IV and apoE, genes in the same gene cluster; CLPTM1, a gene located 3' downstream of apoC-II; MCSF and RPLP0, control genes (**Fig. 2A, left**). Importantly, the size of apoC-II mRNA of the patient was identical to that of normal subjects. Incubation with LXR agonist (T0901317), which is known to upregulate the transcription of genes in the apoE/C-I/ C-II/C-IV gene cluster, increased apoC-II mRNA levels in the cells of both the patient and controls to similar extents (controls, 1.7- and 1.4-fold; patient, 2-fold), indicating that the response to LXR agonist is well preserved in the patient's cells (**Fig. 2A, right**). ApoC-II mRNA levels in the patient's cells were decreased by 53% compared with control cells even in the presence of LXR agonist. As demonstrated by actinomycin D experiment (**Fig. 2B**), the stability of apoC-II mRNA was not different between the patient and normal subject, suggesting that transcription of apoC-II mRNA was impaired in the patient's cells.

Southern Blot and Genomic DNA Copy Number Analyses of the *APOC2* Gene

To rule out the possibility that reduced levels of apoC-II mRNA resulted from a major gene rearrangement, we performed Southern blot analysis (**Fig. 3A**). No difference was observed between the patient and control samples for all enzymes tested except for SacI, which is due to SNP rs5120 in intron 1 (**Table 6**), resulting in SacI digestion in the DNA of the control

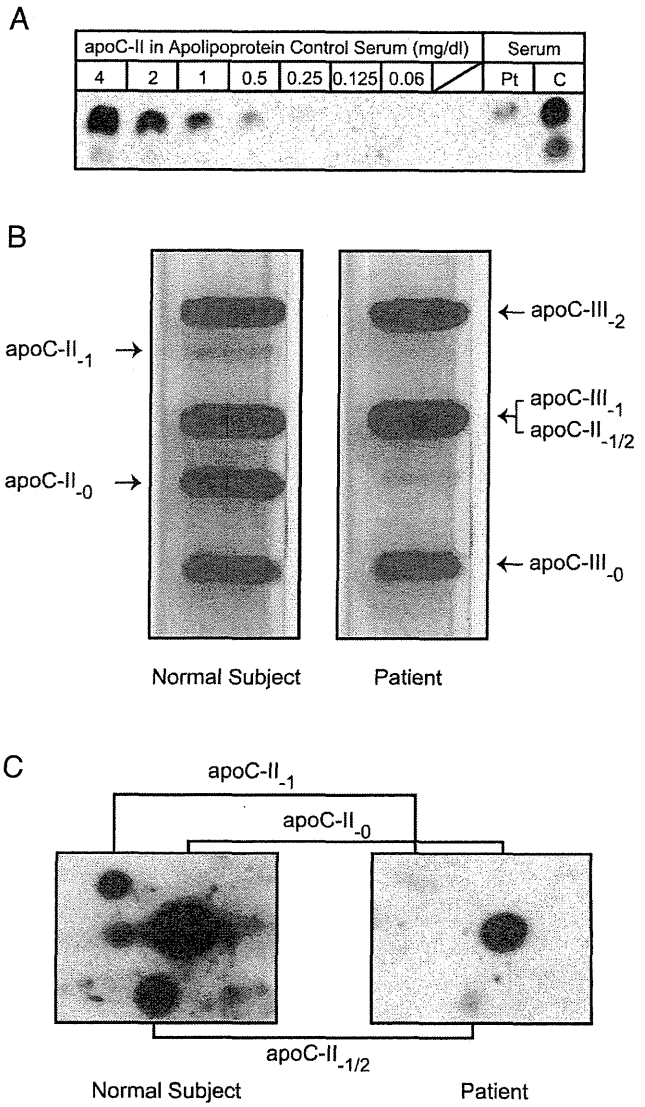

Fig. 1. Plasma apolipoprotein analysis.

(A) Immunoblot analysis of apoC-II. One μL of plasma from the patient (Pt), control subject (C), or apolipoprotein control serum (Daiichi High; Daiichi Pure Chemicals Co., Ltd.) with various concentrations of apoC-II, was subjected to SDS-PAGE followed by immunoblotting using anti-human apoC-II polyclonal antibody. (B) For isoelectric focusing of apolipoproteins, 30 μg of delipidated TGRL apolipoproteins was subjected to electrophoresis using Immobiline DryStrip (pH4-7), followed by Coomassie Brilliant Blue staining. (C) For two-dimensional PAGE of apolipoproteins, 2 μg of delipidated TGRL apolipoproteins was electrophoresed as described in Methods. ApoC-II protein was detected by immunoblotting as described above.

subject but not that of the patient. To exclude the possibility that one of the *APOC2* alleles was missing from the patient's genome, the DNA copy number of the *APOC2* gene relative to the control gene, *RPLP0*, was examined by real-time PCR, revealing no major

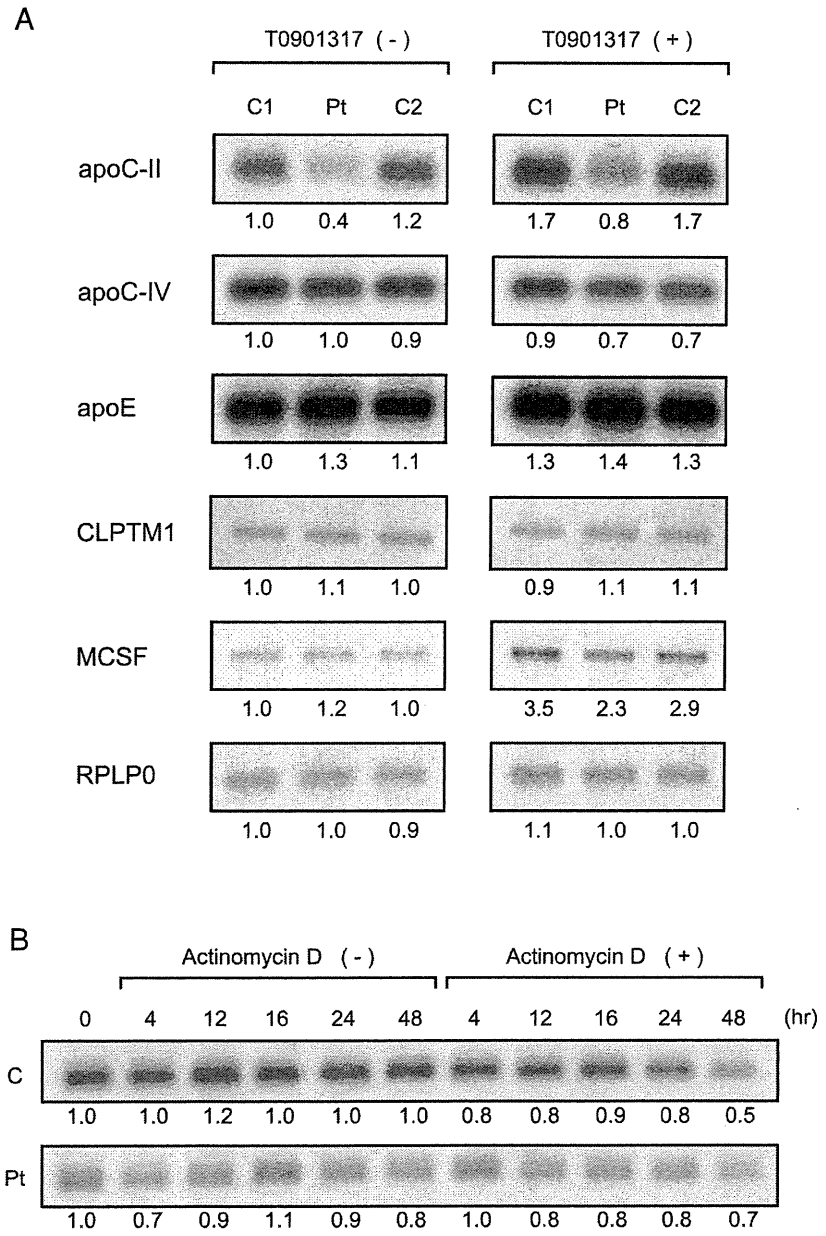

Fig. 2. Northern blot analyses of apolipoproteins in monocytes/macrophages.

(A) Monocytes isolated from peripheral blood of the patient (Pt) and two control subjects (C1 and C2) were plated and differentiated to macrophages. On day 7, cells were incubated with (right panel) or without (left panel) 10 $\mu mol \cdot L^{-1}$ T0901317 (LXR agonist). Cells were harvested the next day to collect mRNA for Northern blot analyses. (B) In a separate experiment, 10 $\mu g \cdot mL^{-1}$ of actinomycin D was added to the incubation medium on day 8 (without T0901317 treatment) to test the stability of apoC-II mRNA. Cells were harvested at the indicated time points. Intensity of each band was quantified by ImageJ 1.39 software (NIH). C, control subject.

difference between the patient and two control subjects (**Fig. 3B**).

APOC2 Minigene Reporter Assay

To determine if decreased apoC-II mRNA transcription in the patient's cells is due to decreased transcriptional activity of the *cis*-regulatory regions of the